ALPHA FOUNDATION FOR THE IMPROVEMENT OF MINE SAFETY AND HEALTH

Final Technical Report

Project Title: Reducing Rib Failure Hazards in Underground Coal Mines by Improvement of the Coal Rib Control System: Integration of Rib Corner, Abutment Loading, and Multiple Seam Interaction

Grant Number: AFCINV24-8

Organization: Missouri University of Science and Technology

Principal Investigator: Taghi Sherizadeh, Ph.D.

Researchers: Cameron Mitchell

Naseer Muhammad Khan, Ph.D.

Contact Information: Department of Mining & Explosives Engineering
226 McNutt Hall, 1400 N. Bishop Avenue, Rolla, MO 65401
573-341-6194, sherizadeh@mst.edu

Period of Performance: September 1st, 2024 – August 31st, 2026

Acknowledgement/Disclaimer: This study was sponsored by the Alpha Foundation for the Improvement of Mine Safety and Health, Inc. (ALPHA FOUNDATION). The views, opinions, and recommendations expressed herein are solely those of the authors and do not imply any endorsement by the ALPHA FOUNDATION, its directors, and staff.

Table of Contents

1.0. Executive Summary 1
2.0. Problem Statement and Objectives 2
3.0. Research Approach and Findings 5
3.1. Objective 1: Conduct Field Surveys and Monitoring of Coal Ribs 6
3.1.1. Task #1. Conducting Field Surveys and Data Collection 6
3.1.2. Task #2. Conduct Field Monitoring for Rib and Corner Response Data 13
3.2. Objective 2: Quantify the Effects of MSI and Abutment Loading on Coal Rib Stability and Evaluate Rib-Corner Stability 24
3.2.1. Task #3. Numerical Model Development 24
3.2.2. Task #4. Quantification of MSI and Abutment Loading Effects on RibFOS and Exploration of Rib-Corner Stability and Support Configurations 29
3.3. Objective 3: Integrate MSI, Abutment Loading, and Rib-Corner Stability into the Coal Rib Control System 47
3.3.1. Task #5. Integration of Project Outcomes into the Rib Support Recommendation Tool (RSRT) 47
3.3.2. Task #6. Field-Case Evaluation of the Updated Rib Support Recommendation Tool (RSRT) 52
4.0. Research Accomplishments 61
4.1 Field Data Collection and Monitoring for Coal Rib Stability Research 61
4.2 Quantified Effects of MSI and Abutment Loading on RibFOS and Advanced Rib-Corner Stability Analysis 61
4.3 Expanded the Coal Rib Control System and RSRT for Complex Loading and Rib-Corner Conditions 62
5.0. Publication Record and Dissemination Efforts 64
6.0. Conclusions and Impact Assessment 65
7.0. Recommendations for Future Work 67
8.0. Acknowledgment 68
9.0. References 69

1.0. Executive Summary

Despite recent efforts and progress to improve coal mine rib stability and hazard mitigation, rib-related fatalities and injuries persist in the coal mining industry due to numerous factors and hazards. Critically, rib instabilities and failures initiated by multiple seam interactions (MSI), abutment loading conditions, and coal rib corners are important contributing factors to these persistent injuries and fatalities. To date, no established methodology or design tool can account for these hazard sources and their effects on coal rib stability, forcing coal mine operators to rely on trial-and-error or legacy practices to manage these risks. Therefore, an engineering-based design tool that accounts for these risks and facilitates effective coal rib design and support planning is necessary to improve coal rib stability in U.S. underground coal mining operations.

In response to this need, this research effort was organized into the following six tasks: i) conducting extensive coal rib surveys and data collection, ii) conducting field monitoring at a selected active room-and-pillar coal mine, iii) developing numerical modeling approaches to evaluate the impacts of MSI and abutment loading on coal rib stability and to assess rib-corner stability, iv) conducting parametric modeling studies to quantify relationships between coal rib stability and MSI, abutment loading, and rib-corner conditions, v) incorporating the developed relationships and methodologies into the coal rib control system, and vi) field-case validation of the enhanced coal rib control system. The field surveys and monitoring expanded the empirical database of coal rib behavior under complex mining conditions and informed the numerical modeling effort. The numerical studies generated synthetic data spanning a range of mining and geological conditions and were used to quantify the effects of MSI and abutment loading on coal rib stability and to investigate rib-corner behavior and support.

A direct linkage was established between the NIOSH-developed Analysis of Coal Pillar Stability (ACPS) software and the coal rib control system, allowing estimated MSI-induced vertical stress increases to be incorporated into rib-stability evaluations. Numerical analyses of side- and face-abutment loading established relationships between these loading conditions and rib factor of safety (RibFOS), while three-dimensional modeling extended the established rib-scale methodology to investigate pillar-corner response and evaluate potential corner-support configurations. Together, these analyses expanded the coal rib control framework beyond development-stage mid-rib conditions to address additional loading and geometric conditions encountered in underground coal mines.

The developed relationships linking coal rib stability to MSI and abutment loading, together with preliminary coal rib corner stability analyses and support guidance, were incorporated into the Rib Support Recommendation Tool (RSRT) to facilitate efficient analysis of coal rib stability under various mining and geological conditions. Following the integration of the developed relationships and recommendations, the updated tool was initially assessed using two active-mine cases exposed to MSI and abutment loading conditions and compared with documented field conditions and support practices. The tool successfully matched or exceeded the active rib support design for a mine experiencing significant MSI effects and a separate mine subjected to substantial abutment loading conditions. These applications demonstrate the expanded coal rib control system's ability to address complex loading conditions and provide improved support guidance. This strengthens its practical value for coal rib design and advancing its potential to improve rib safety in U.S. underground coal mines.

2.0. Problem Statement and Objectives

Coal rib control is a critical aspect of underground coal mining safety, as rib failures remain a significant ground control hazard and continue to result in injuries and fatalities in U.S. underground coal mines (Guner, Nowak, et al., 2023). Coal rib stability is expected to become increasingly challenging as mining extends to greater depths and encounters more complex stress conditions, including multiple seam interactions (NIOSH, 2019). In response to this persistent hazard, Missouri S&T researchers have continued to develop and refine an engineering-based coal rib control system and the Rib Support Recommendation Tool (RSRT) to improve the assessment of rib stability and support requirements across a range of mining and geological conditions. Prior advancements expanded the system's capability to evaluate mid-rib stability under a broad range of geological and mining conditions; however, important limitations remained under more complex loading and geometric conditions.

Geologic conditions and mining environments vary widely across U.S. underground coal mines, and no standardized methodology or systematic guideline currently exists for coal rib stability assessment and support design. This gap leaves mine operators to rely on trial-and-error and local or legacy practices for designing rib support systems (Mohamed et al., 2016). In response to this gap, researchers at NIOSH and Missouri S&T have conducted extensive field, numerical, and empirical studies to quantify the integrity of coal pillar ribs and aid mine operators with an engineering-based coal rib design approach (Sherizadeh, 2023; Sherizadeh et al., 2024).

Prior to the present project, the developed coal rib control system could evaluate the condition of both solid coal ribs and ribs with rock partings. Mine professionals could determine the Coal Pillar Rib Rating (CPRR) and unsupported rib factor of safety (RibFOS) for site-specific mining conditions using the developed tables and charts incorporated into the coal rib control system. Utilizing these charts and tables, mining professionals could quantitatively assess the stability of the unsupported mid-span regions of the rib during the development stage, particularly in cases with no multiple seam interaction (MSI). To facilitate practical use of the developed system, a graphical user interface-based software for coal rib support design was developed. The developed equations, charts, and tables were integrated into this application, simplifying the steps necessary for a mine operator to evaluate coal rib stability during development and design effective rib support patterns.

Building on these advancements, the next stage in developing the coal rib control system focused on expanding its capabilities to address more complex rib conditions. Extensive field observations and analysis of MSHA fatality reports identified important factors for further incorporation into the system: rib corners, abutment loading conditions, and multiple seam interactions (MSI). The importance of addressing these factors is further supported by the MSHA "Roof Control and Ground Support Plan Review Procedures" handbook, which identifies these three factors as "contributing factors to rib fall fatalities" (MSHA, 2020). Figure 1 summarizes the analysis of MSHA rib-related fatality reports from 2012 to 2022 in terms of rib-failure location, mining stage, and MSI potential. Rib corners are particularly important because higher stress levels and multiple

free surfaces increase the likelihood of sloughing and failure. Recent MSHA reports indicate that rib corner failures account for the majority of rib-failure-related fatalities, underscoring the need for comprehensive rib corner control strategies. Furthermore, abutment loading conditions can significantly impact rib stability in longwall and retreat room-and-pillar mines, while MSI can introduce additional stress concentrations in multiple seam mining operations. These factors have been implicated in a significant portion of rib-related fatalities, providing further motivation to expand the capabilities of the coal rib control system.

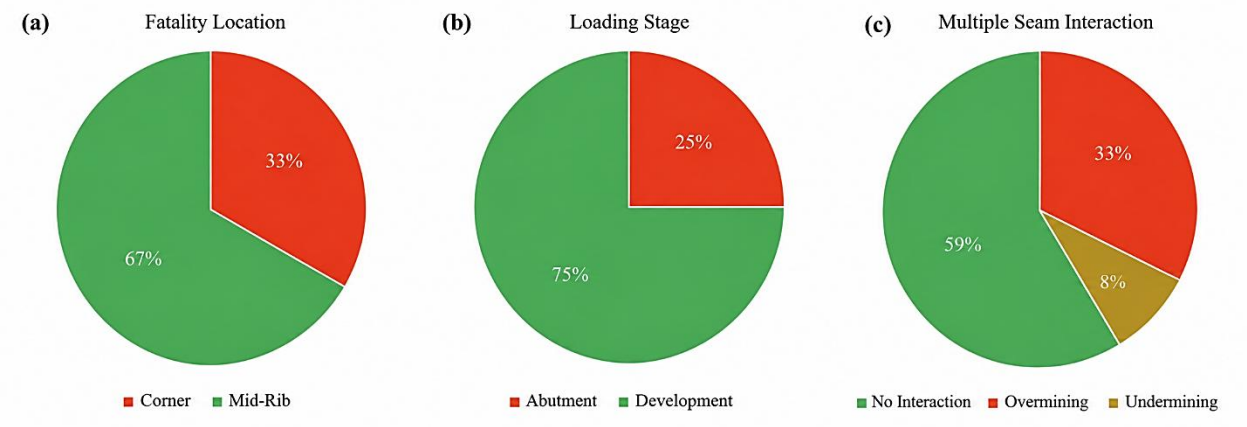


Figure 1: MSHA rib-related fatality reports analysis from 2012 to 2022, based on (a) rib failure location, (b) mining stage, and (c) multiple seam interaction potential.

The following subsections discuss each of these factors in greater detail, with emphasis on their influence on coal rib stability and their relevance to the continued development of the coal rib control system.

Rib Corners

The CPRR and coal rib control system have been developed and updated based on a combination of empirical field datasets and synthetic data from numerical parametric studies. The main focus of previous coal rib control system development efforts was to assess stability within the mid-span regions of the rib and provide initial support recommendations for areas not significantly influenced by stress concentrations near pillar corners. Given the localized stress concentrations in the pillar corners and the presence of two free surfaces, sloughing is expected to occur to a greater extent in these areas than in the mid-span regions. This has been consistently observed during site visits, where the pillar corners are more susceptible to sloughing and failure than the mid-span areas. Accordingly, rib-corner instability represents a significant hazard that must be carefully evaluated and managed in underground coal mining operations. The MSHA reports on rib fall-related fatalities further support the significance of this hazard. Specifically, rib-failure-related fatality reports from 2019 to 2022 indicate that rib corner failures were responsible for four out of the five reported fatalities, demonstrating the critical importance of addressing and mitigating risks associated with rib corner stability. Further analysis of rib-failure-related fatality reports from 2012 to 2022 showed that one-third of the fatal incidents occurred at rib corners (Figure 1a). In addition, MSHA fatality analysis conducted by Jones et al. (2014) for 1996 to 2013,

combined with additional analysis of MSHA fatality reports from 2014 to 2022, indicated that 16 of 24 corner-related fatalities occurred within 10 ft of the coal pillar corner. These data underscore the elevated risk associated with rib-corner instability and the need for targeted corner-control strategies in underground coal mines.

Abutment Loading Conditions

While the coal rib control system was initially developed to primarily assess rib stability under development loading conditions, rib loading can change substantially as mining progresses. In retreat room-and-pillar and longwall mining, extraction redistributes stresses to the remaining pillars and adjacent coal ribs, creating abutment loading conditions that can increase the potential for rib instability. In retreat room-and-pillar mining, removal of adjacent pillars transfers additional load to the remaining pillars, while advancement of a longwall face generates face and side abutment stresses along the surrounding gateroads. These stresses can become particularly concentrated near the intersections of the longwall face and gateroads, where face and side abutment loading interact. Abutment loading has also been shown to increase the depth of fracturing in adjacent coal ribs (Zhang et al., 2017). Despite the fact that approximately 75% of rib-failure-related fatalities analyzed from MSHA reports occurred under development loading conditions, it remains critical to integrate mine-induced stress conditions into the coal rib control system (Figure 1b). This integration will enable the system to evaluate rib stability under both development and abutment loading conditions. By including this capability, the rib control system can better account for changes in rib stability as mining-induced stresses evolve.

Multiple Seam Interaction (MSI)

Many underground coal mines face complex ground-control conditions associated with multiple seam interactions caused by mining above or below previously mined workings. Moreover, coal rib stability can become increasingly challenging as mining extends to greater depths and encounters additional stress concentrations associated with MSI. In both undermining and overmining situations, the roof, rib, and floor have the potential to interact with old workings when the overburden-to-interburden thickness (OB/IB) ratio is sufficiently high; an OB/IB ratio greater than 5 has been identified as an indicator of potential interaction (Zipf, 2005).

Mine planners and regulators in the U.S. commonly utilize the Analysis of Multiple Seam Stability (AMSS) methodology to assess the risks associated with potential interactions between multiple coal seams (Mark et al., 2007b). AMSS was developed using 356 multiple-seam case histories and evaluates the potential severity of MSI. The results are categorized into three risk levels: Green, indicating a major interaction is unlikely; Yellow, suggesting that adding a pattern of cable bolts or other equivalent supplemental support could significantly reduce the likelihood of a major interaction; and Red, where a major interaction is considered likely (Mark, 2021). These categories are primarily intended for assessing multiple-seam effects on pillar stability and do not directly quantify their effects on coal rib stability.

While the impact of MSI on rib stability is acknowledged, the existing literature in this field is largely based on field observations and provides limited quantitative guidance for evaluating its effect on coal ribs. The MSHA fatality analysis conducted for this study further illustrates the potential relevance of MSI to rib hazards. Approximately 41% of the evaluated rib-failure-related fatalities were associated with potential multiple-seam interaction conditions, including both overmining and undermining cases (Figure 1c). These observations highlight the need to establish a quantitative link between MSI-induced stress changes and coal rib stability and incorporate these effects into the coal rib control system.

Research Objectives and Expected Impact

The evidence presented above demonstrates the importance of rib corners, abutment loading conditions, and multiple seam interactions to coal rib stability. Although approximately 75% of the analyzed rib-failure-related fatalities occurred under development loading conditions, loading stage represents only one aspect of the conditions that defined the applicability of the previously developed coal rib control system. When rib-failure location, loading condition, and MSI potential were considered collectively, the existing system could address approximately 25% of the conditions associated with the fatal incidents analyzed. These findings provided the basis for the present research. The research effort was structured around three overarching objectives:

1. Conduct field surveys and monitoring of coal ribs to expand the database of field observations and measurements used to support development of the engineering-based coal rib control system.
2. Quantify the effects of MSI and abutment loading on coal rib stability through parametric numerical modeling and evaluate rib-corner stability using three-dimensional numerical models.
3. Integrate MSI, abutment loading, and rib-corner stability into the coal rib control system to expand its capabilities for mitigating rib hazards in underground coal mining.

The major expected impact of this research is to expand the applicability of the engineering-based coal rib control system to more complex mining and loading conditions. The expanded system is intended to enable more comprehensive rib stability assessments and provide improved support recommendations across a wider range of underground coal mining conditions. This expanded capability is expected to improve rib stability assessment, support design, and hazard mitigation in underground coal mines.

3.0. Research Approach and Findings

To continue developing and refining the coal rib control system, the Missouri S&T research team conducted an extensive study to improve the understanding of the effects of MSI and abutment loading on coal rib stability and to evaluate rib-corner stability and potential support configurations. The research combined field surveys and monitoring data with numerical modeling approaches, building on methodologies developed in previous research to explore the complex mechanisms affecting coal rib stability. A 50-day coal rib monitoring study was conducted along with surveys of 8 active coal mines across 7 coal seams. The data collected from the field

monitoring and surveys expanded the database of coal rib behavior and responses under a range of mining and geological conditions. These field data and observations were considered alongside numerical modeling and parametric analyses to evaluate coal rib behavior under various scenarios and conditions. The parametric study results were then used to establish quantitative relationships linking MSI and abutment loading to coal rib stability, while field observations informed the investigation of rib-corner behavior, and three-dimensional numerical modeling was used to evaluate rib-corner stability and investigate potential support configurations. These relationships and findings were incorporated into the coal rib control system and implemented in the RSRT, with the objective of providing coal mine operators with an effective engineering tool to facilitate coal rib stability assessment and support design decisions across various coal mining environments.

To meet the objectives of this research project, the research efforts were segmented into six main tasks to address the main challenges observed in complex coal mine environments. These tasks also supported the development of a methodology for coal mine operators to link outputs from established coal mine engineering design tools with the expanded coal rib control system.

Task 1 involved extensive coal mine site surveys to collect information on coal rib and rib-corner conditions in various complex mining environments, with a focus on MSI and abutment loading effects. Task 2 encompassed selecting an appropriate instrumentation site, followed by installing monitoring equipment in an active coal mine to collect data on coal rib behavior during retreat mining operations. Task 3 focused on developing numerical modeling approaches, building on previously calibrated 2D models, to represent rib response under different mining environments and conditions. Task 4 involved parametric analysis of various mining and geological conditions, along with evaluation of rib-corner stability and support scenarios, to generate the necessary inputs for expanding the coal rib control system. Task 5 entailed incorporating the developed MSI and abutment-loading relationships and preliminary rib-corner support guidance into the coal rib control system and implementing these capabilities in the RSRT. Task 6 concluded the research efforts by evaluating the updated coal rib control system and RSRT against 2 field cases selected from the completed site surveys, representing MSI and abutment loading conditions.

The following sections detail the specific research tasks and provide an overview of the background, methodologies, and analytical approaches utilized to achieve the objectives outlined in the Problem Statement and Objectives section.

3.1. Objective 1: Conduct Field Surveys and Monitoring of Coal Ribs

3.1.1. Task #1. Conducting Field Surveys and Data Collection

To expand the research team's database of coal rib responses under various mining and geological conditions, our research team conducted field surveys of coal pillar ribs and corners at 8 different active coal mines. These mining sites covered 7 different coal seams: Herrin No. 6, Indiana No. 5, Pocahontas No. 3, No. 2 Gas, Lower Kittanning, Williamson, and Eagle, providing our team with observations of pillar-rib and corner behavior across a range of mining and geological conditions.

During the site visits, surveys were conducted on at least 4 different pillars for each seam. Additionally, the corner conditions of neighboring pillars adjacent to the surveyed pillars were documented to provide a broader understanding of rib and corner conditions.

To ensure consistency with previous research, the rib surveys utilized a data collection sheet developed in a recently completed project. Furthermore, critical parameters, such as interburden thickness, the presence of a remnant structure (whether an isolated remnant pillar or a gob-solid boundary), and the type of interaction (undermining or overmining), were documented to characterize potential MSI conditions.

Herrin No. 6 Seam

The rib survey was initially conducted in the Herrin No. 6 seam, which was identified as having the most favorable rib conditions among all seams surveyed. The Herrin No. 6 seam, also known as the Herrin coal, is a major economic coal seam in Illinois that averages about 6 feet in thickness and underlies a large part of southern and west-central Illinois. A total of 5 pillars were surveyed within this seam, which is mined using multiple continuous miners. Notably, no evidence of MSI was identified, and pillar retreat mining is not implemented in this mine. The overburden depth above the surveyed pillars ranges between 250 and 300 feet, with the mining height varying between 6 and 7.5 feet. Pillar dimensions show variability, ranging from 40×40 feet to 60×100 feet. The immediate roof strata are composed of moderate shale and limestone, while the immediate floor consists of fireclay. Given the shallow overburden and coal strength ranging from 3000 to 3500 psi, rib support is not used in the survey area. The coal seam thickness in this area reaches up to 6.5 feet. Despite the overall stability of the ribs and corners, localized floor heave was observed in a specific section where ponded water was present on the mine floor and affected the moisture-sensitive fireclay. The floor heave induced more than slight skin damage to the rib corners, with rib sloughage reaching up to 1 foot in certain pillar corners. Although the observed rib sloughage was localized and limited, the observations indicate that ponded water on the mine floor can adversely affect the moisture-sensitive fireclay and contribute to localized floor heave and associated rib-corner deterioration. These conditions could also affect long-term rib stability.

Indiana No. 5 Seam

The Indiana No. 5 coal seam, also known as the Springfield seam, is the most significant and extensively mined coal seam in the Eastern Interior Basin, with thicknesses ranging from 4 to 9 feet in some areas and averaging approximately 6 feet. A total of 4 pillars were surveyed within this seam. Coal is mined using the room-and-pillar method in the 4 active units. There are no old workings underlying or overlying the seam, and pillar retreating has not been implemented in this mine. The overburden depth above the surveyed pillars ranges between 250 and 350 feet, with the mining height varying between 75 and 95 inches. The average coal thickness is around 50 inches. Pillar dimensions are relatively consistent in this mine, with uniform 60×60 ft square pillars. The immediate roof and floor strata consist of black and dark gray shale. Coal strength ranges from 1,500 to 2,000 psi. Due to the shallow overburden and absence of pillar retreating, rib support is

not used in the surveyed area. Although rib and corner sloughage generally remained minimal, with observations of 3 inches or less, in the return airway mains, where one of the pillar surveys was conducted, the effects of airflow contributed to increased rib sloughage. The rib sloughage reached approximately 1 foot in the mid-span of the rib, while corner failures reached up to 1.5 feet. Figure 2 presents representative images of the surveyed pillar corner within the return airway mains.

The uppermost member of the rib, composed of shale with an approximate compressive strength of 4,000 psi, remained intact, whereas the weaker coal at the rib corner failed along its weak interface with the overlying shale, resulting in brow formation. No tension cracks were observed in the formed brows at the corners. Based on the shale strength, brow depth, and overburden conditions, the observed brow was considered stable under the conditions at the time of the survey.

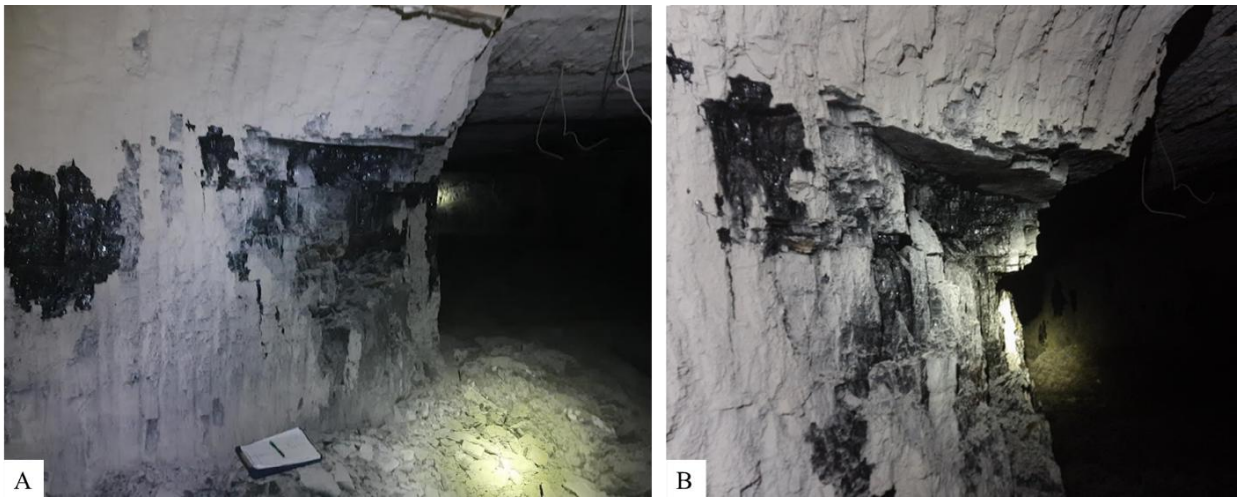


Figure 2: (A) General view of the pillar corners in the Indiana No. 5 seam return airway mains and (B) close-up view of the failed coal and formed brow, with a depth of approximately 1.5 feet.

Pocahontas No. 3 Seam

The Pocahontas No. 3 coal seam, part of the Lower Pennsylvanian Pocahontas Formation, exhibits a thickness ranging from 2 to 11 feet and covers approximately 650 square miles in southern West Virginia. A total of 5 pillars were surveyed within this particular seam. The coal seam is mined using the room-and-pillar method, with pillar retreating implemented in the 5 active sections. These active sections are approximately 300 feet below the previously mined Beckley seam, with an OB/IB ratio of approximately 4. Based on survey observations, no evidence of multiple-seam interaction was identified, as expected. Rib height generally varies between 6 and 10 feet, leading to variability in pillar dimensions. The immediate roof and floor primarily consist of moderate to strong shale. The rib comprises 5 to 6 distinct units, including 2 shale partings that are more competent than coal, with compressive strengths ranging from 2,500 to 3,000 psi. In contrast, coal itself is extremely weak. While previous laboratory tests and literature indicate coal strength in the range of 1,000 to 1,500 psi, in some areas, the coal is weak enough to be broken by hand. Due to

this weakness, rib bolting cannot be effectively applied directly to the coal and is instead installed in the shale partings.

Two rows of 5-foot-long, ¾-inch-diameter, Grade 60, fully grouted rib bolts are installed at 4-foot spacing. The upper shale bolts are typically installed at an angle of 20–30 degrees. A 12×12-inch face plate is used. Systematic rib bolting is also applied at the corners, and if immediate failure is observed post-excavation, additional bolts are installed as necessary. In some cases, bolt spacing of less than 2 feet was observed in highly deteriorated corners. Across all surveys conducted in this seam, rib sloughage levels at pillar corners were found to be 1.5 to 2 times greater than those observed at the mid-span of the rib. Rib sloughage in the mid-span generally ranged between 1 and 2 feet, whereas corner sloughage reached 2.5 to 3 feet. Rib corner sloughing of up to 4.5 feet was observed in many pillars during retreat mining due to elevated stresses near the pillar line caused by abutment loading.

No. 2 Gas Seam

The No. 2 Gas coal seam, part of the Kanawha Formation in the Appalachian Basin, exhibits variable thickness ranging from 1 to 7 feet and is often associated with challenging roof conditions due to the presence of rider coals. This seam is typically mined using the room-and-pillar method with pillar retreating. A total of 4 pillars were surveyed within this particular seam. The overburden depth at the surveyed pillars is approximately 1,100 feet, with an interburden thickness of about 130 feet between the No. 2 Gas seam and the Alma seam. According to the Analysis of Coal Pillar Stability (ACPS) program (Mark & Agioutantis, 2019), the critical interburden thickness required for multiple-seam interactions to occur is 84 feet during the development stage and 131 feet during the pillar retreat stage. Given that the interburden thickness at the study site exceeds the development-stage critical value and is approximately equal to the critical value during pillar retreat, no significant multiple-seam interaction was expected based on the ACPS assessment. Observations at this survey site did not indicate notable multiple-seam interaction effects.

The immediate roof and floor primarily consist of strong shale. The rib comprises 4 distinct units, including 2 shale partings that are more competent than coal, with compressive strengths ranging from 3,500 to 4,500 psi. In contrast, the coal is moderately strong. Previous laboratory tests and literature indicate coal strength in the range of 2,000 to 2,500 psi. The mine extracts approximately 2 to 3 feet of shale from the immediate roof, resulting in a total mining height of about 6 to 7 feet. This rib configuration has the potential to form rib brows, particularly near pillar corners, as observed in several locations (Figure 3). To improve the stability of the rock parting, rib bolts are systematically installed during the mining cycle in all entries. A single row of fully grouted, Grade 60, 5-foot-long angled rib bolts is installed in the top rock parting when its thickness exceeds 2 feet. These bolts are accompanied by 6×6-inch steel plates and 12×12-inch plywood plates for additional support. The installed bolts are spaced approximately 6 to 8 feet apart, as shown in Figure 3.

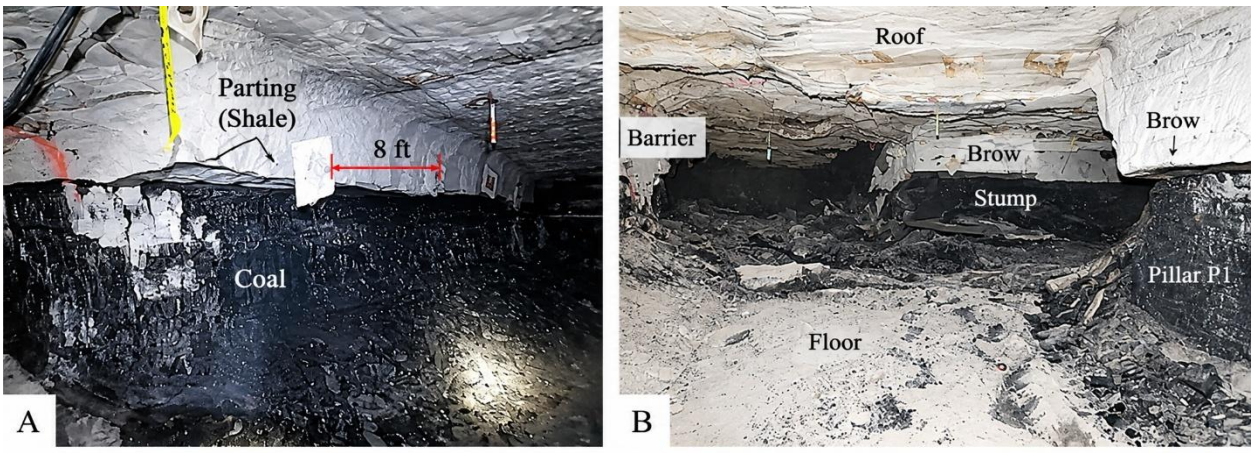


Figure 3: Rib conditions at the No. 2 Gas seam: A) During development, B) Under abutment stress.

Lower Kittanning Seam

The Lower Kittanning Seam primarily consists of a single coal horizon with a bone coal parting. Due to the coal reserve characteristics, the mine operates using both longwall and continuous mining methods, with 4 continuous miners and one longwall section in operation. The coal seam thickness ranges from 4 to 6 feet, averaging approximately 5 feet. A total of 4 pillars were surveyed within this seam. The overburden depth above the surveyed pillars varies between 300 and 450 feet, with the mining height ranging from 95 to 110 inches. The active longwall panel is 1,100 feet long, and the maximum horizontal stress orientation is west-east (W-E). The immediate roof consists of strong shale, while the floor is moisture-sensitive fireclay, which is prone to floor heave in certain areas. The rib structure generally consists of 3 to 4 distinct units. In some locations, the shales divide the coal seam into two separate units with coal streaks and shale partings. The uppermost rib unit consists of 1 to 2 feet of shale. The coal strength ranges from 1,750 to 2,250 psi, while the shale parting has an approximate strength of 4,000 psi. Overall, no significant rib or roof stability issues have been observed in the mine. However, small-scale floor heaving problems have been reported in certain areas due to the presence of fireclay in the floor lithology.

In line with previous field observations, rib support is implemented in the mine despite the shallow overburden depth and relatively strong rib conditions, given the use of longwall mining. Although the MSHA-approved roof control plan only recommends spot bolting at rib corners extending 4 feet, the company has adopted a systematic rib support approach. A two-row pattern of fully grouted, Grade 60, 5-foot-long rib bolts is installed 3 feet below the roof line and 3 feet above the floor line. These bolts are accompanied by 8×8-inch steel plates and 10×30-inch rectangular surface support plates for skin control. The installed bolts are spaced approximately 6 to 8 feet apart. Across all surveys conducted in this seam, rib sloughage levels at the mid-span of the rib and at the pillar corners were very similar, with skin damage generally limited to less than 6 inches. No multiple-seam interaction (MSI) was observed. To further assess face and side abutment conditions, field observations were conducted within the active longwall panel. The rib conditions were generally good, with slightly increased sloughing near the roof line.

Williamson Seam

The Williamson coal seam, part of the Kanawha Formation in the Appalachian Basin, is typically found between the Coalburg seam at the top and the Eagle seam at the bottom, within an interval containing over 10 coal seams. Rib surveys were conducted in 2 different mines operating within this seam, with one examined under development conditions and the other during pillar retreat operations. The mined coal seam thickness ranges between 40 and 52 inches, with a mining height varying from 60 to 100 inches. Pillar dimensions are generally 40×80 feet, and the overburden depth varies between 300 and 450 feet. The immediate roof and floor consist of strong shale, and the rib is composed of 3 to 4 distinct units, with sloughage initiating at the weak contact between the uppermost shale and coal. No published rock mechanics testing data were identified for the coal properties of the Williamson seam. However, Schmidt hammer tests conducted in the field during the site survey estimated coal strength between 2,000 and 2,500 psi.

Mining is currently conducted over previously extracted Powelton seam panels. Despite the interburden thickness exceeding 100 feet, which generally limits multiple-seam interactions considering the overburden depth, the effects of underlying solid remnant structures were observed, particularly at pillar corners during the development stage. In several pillar corners, rib sloughage reaching up to 2 feet was observed, and nearly all pillars located above the solid remnant structure exhibited apparent cracks ranging from 1 to 2 feet in depth at their corners. However, due to the shallow overburden and strong rib units, no rib support system is implemented in the mine. In the retreat panel, rib surveys and observations indicated that sloughage at pillar corners began approximately 2 to 3 pillars ahead of the retreat zone, where no remnant structure was present. The corner sloughage levels of pillars adjacent to the retreat area reached up to 1.5 feet, while the mid-span of the rib generally remained in good condition, even in pillars neighboring the retreat zone. Only localized, very slight skin damage of approximately 3 inches was observed at the mid-span of the rib.

The surveys and visual observations conducted in this seam were highly valuable, as they documented the effects of abutment loading on pillar corners and revealed unexpected signs of MSI, despite initial expectations that significant MSI would not occur. These observations indicated that, despite favorable mining and geological conditions, the coal pillar corners showed greater sensitivity to localized stress concentrations associated with MSI and abutment loading. Although the mid-rib regions of the surveyed pillars were in good condition, consistent corner instability was observed across the surveyed region.

Eagle Seam

The Eagle coal seam extends throughout the Central Appalachian Basin, particularly in southern West Virginia, and is part of the Kanawha Formation within the Pennsylvanian system, with a thickness ranging from 15 to 72 inches (averaging 46 inches). The mine has a single active section using 2 continuous miners to extract coal. The coal seam thickness ranges from 40 to 55 inches, averaging around 50 inches, while rib height typically varies between 7 and 8 feet. The

immediate roof and floor primarily consist of strong shale and moderately sandy shale. The rib comprises 4 distinct units, with the uppermost unit consisting of 1 to 2 feet of shale. The coal itself is weak and is divided into 2 separate units by a 1 to 2 ft shale parting, with a strength range of 1,500 to 2,000 psi. Previous laboratory tests and literature indicate that coal strength generally falls within the 1,250 to 1,500 psi range. A total of 5 pillars were surveyed within this seam, all within the same section, and rib sloughage mapping was conducted across more than 100 pillars. The mine presents 2 unique characteristics that make the collected data particularly valuable: (i) The surveyed panel is located beneath steep and rugged mountainous terrain, leading to significant variations in overburden depth, ranging from 400 to 1,100 feet within the same section (Figure 4); and (ii) a portion of the panel lies just 30 feet above a previously mined seam (Upper Eagle).

Due to the varying conditions within the mine, there is no consistent rib support plan in place. The mine utilizes fully grouted, Grade 60, 5-foot-long rib bolts with a 5/8-inch diameter. In areas with lower overburden depth and minimal multiple-seam interaction, a single row of rib bolts is installed at the mid-rib with 6 to 8 ft spacing. Under more severe conditions, a two-row bolting system is used with tighter 4 ft spacing, with bolts placed in both the upper and lower sections of the coal unit. Since the uppermost shale is stronger than the coal, numerous formed brows have been observed in the surveyed section. Particularly in areas where bolts were installed with 6- to 8-foot spacing, the thickness of the formed brows reached up to 2 feet. In such cases, additional timber support was implemented to support the brows and improve overall rib stability.

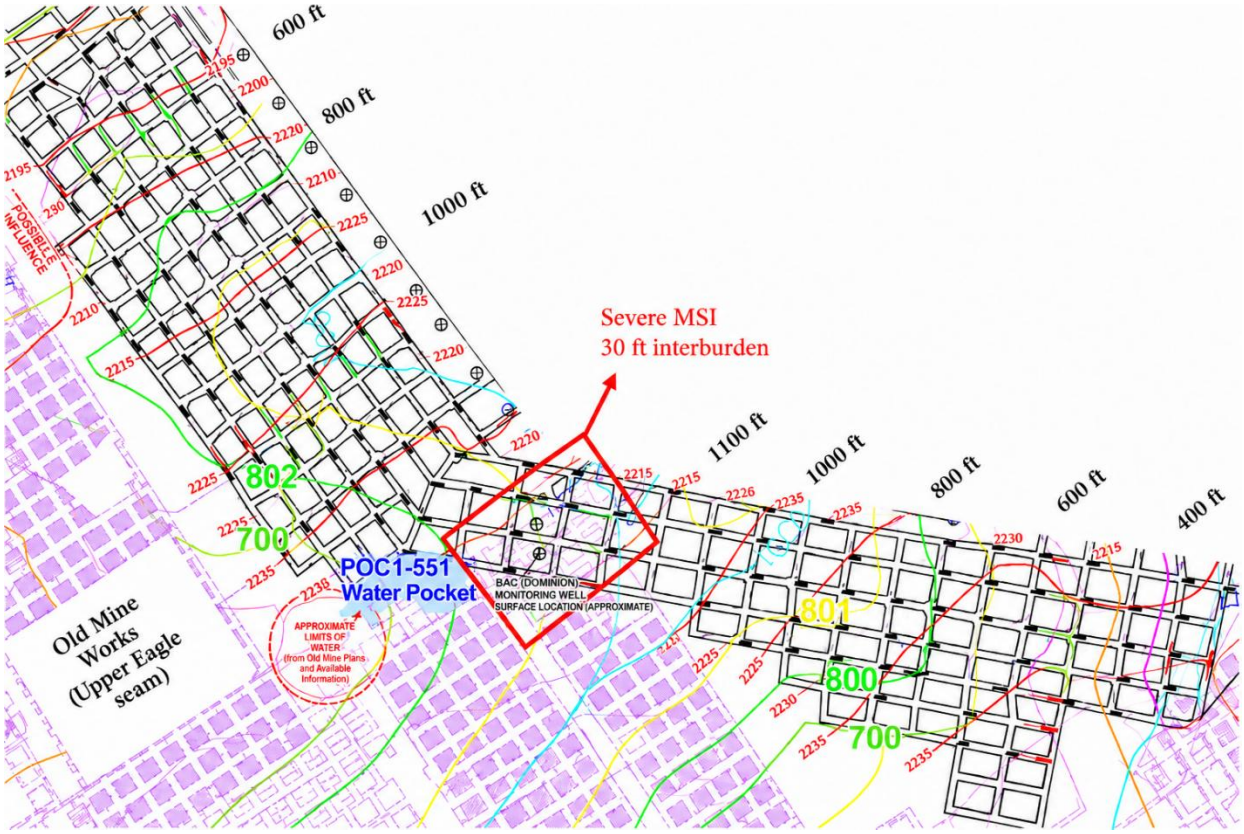


Figure 4: Studied section in the Eagle Seam. The area experiencing severe MSI, with a 30 ft interburden to the previously mined Upper Eagle Seam, is highlighted in red. Overburden depth in this section ranges from 400 ft to 1,100 ft.

Among all the surveyed seams, this seam exhibited the most complex rib behavior. A clear relationship between increasing overburden depth and rib deterioration was observed, although MSI also influenced conditions within portions of the surveyed panel. In areas with low overburden depth (Figure 4), rib sloughage remained minimal, typically 3 inches or less, even at pillar corners. However, in regions where the overburden depth exceeded 1,000 ft, rib sloughage increased significantly, reaching nearly 50 inches.

The significant variability in mining and geological conditions at this survey location was consistent with observations made across the other site surveys regarding the greater sensitivity of pillar corners to elevated and concentrated stresses. Pillar corners showed greater deterioration under conditions associated with abutment loading and MSI. Across the surveyed mine sites, corner degradation was generally more pronounced than damage observed in the mid-rib regions.

3.1.2. Task #2. Conduct Field Monitoring for Rib and Corner Response Data

Instrumented Site Overview

The selected monitoring site is an underground coal mine located in West Virginia, where the Alma seam is extracted using the room-and-pillar method. To optimize coal recovery, pillar retreat mining is implemented. During initial site visits to prepare for instrumentation, the research team

observed that the mine extracts approximately 2 to 3 feet of shale from the immediate roof and 3 to 6 inches from the floor, resulting in a total mining height of approximately 6 feet. The coal seam is approximately 3 feet thick at the instrumented pillar location. Figure 5 shows the rib lithological profile measured at the instrumented pillar. The instrumented pillar's dimensions were measured as 115 ft (entry) by 70 ft (crosscut) centers, with an excavation width of approximately 15 ft. The pillar location was estimated to be under approximately 700 ft of overburden with an interburden thickness of 180 ft between the Alma seam workings and the overlying remnant structures in the Cedar Grove coal seam.

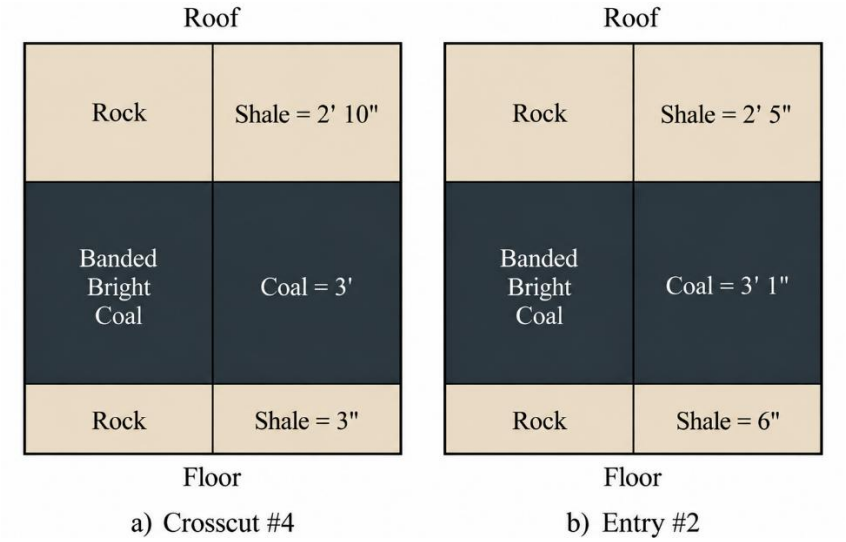


Figure 5: Rib profiles for the instrumented pillar (not to scale).

The uniaxial compressive strengths (UCS) of the rock parting and coal seam were estimated using Schmidt hammer rebound tests conducted on the rib of the instrumented pillar. The average Schmidt hammer rebound numbers (N) recorded were 38 for the rock parting and 35 for the coal seam. These rebound values were then applied to Equation (1) (Saptono et al., 2013) for the rock parting and Equation (2) (Rashed et al., 2018) for the coal seam to estimate the uniaxial compressive strengths, respectively. Based on these calculations, the estimated UCS values were about 5,000 psi for the rock parting and 3,400 psi for the coal seam.

$$UCS\ for\ shale\ (psi) = 44.66 \times N^{1.327} \quad (1)$$

$$UCS\ for\ coal\ (psi) = 215.7 \times N - 3779 \quad (2)$$

Although the rib configuration has the potential to form rib brows, their occurrence was limited to a few pillar corners due to the coal's relatively high strength. Rib bolting is conducted on cycle in all entries, using a single row of 5-foot-long, 5/8-inch diameter, Grade 60, straight, fully grouted rib bolts installed within the middle of the top rock parting. Each rib bolt is secured with 6×6-inch steel plates and 12×12-inch plywood plates, with an average spacing of 8 feet between bolts.

The instrumentation site was selected to investigate stress transfer effects during pillar retreat mining and to assess the impact of remnant structures on rib performance within the Alma seam. The selected panel is characterized by large remnant structures (see Figure 6) directly overhead, with an interburden thickness of approximately 180 feet. The instrumented pillar is located between entries 2 and 3 and crosscuts 4 and 5 within the B-2 panel. A mine map depicting the location of the instrumented pillar is shown in Figure 6. The B-2 panel, where the study was conducted, underwent rapid development and retreat operations due to its relatively short panel length.

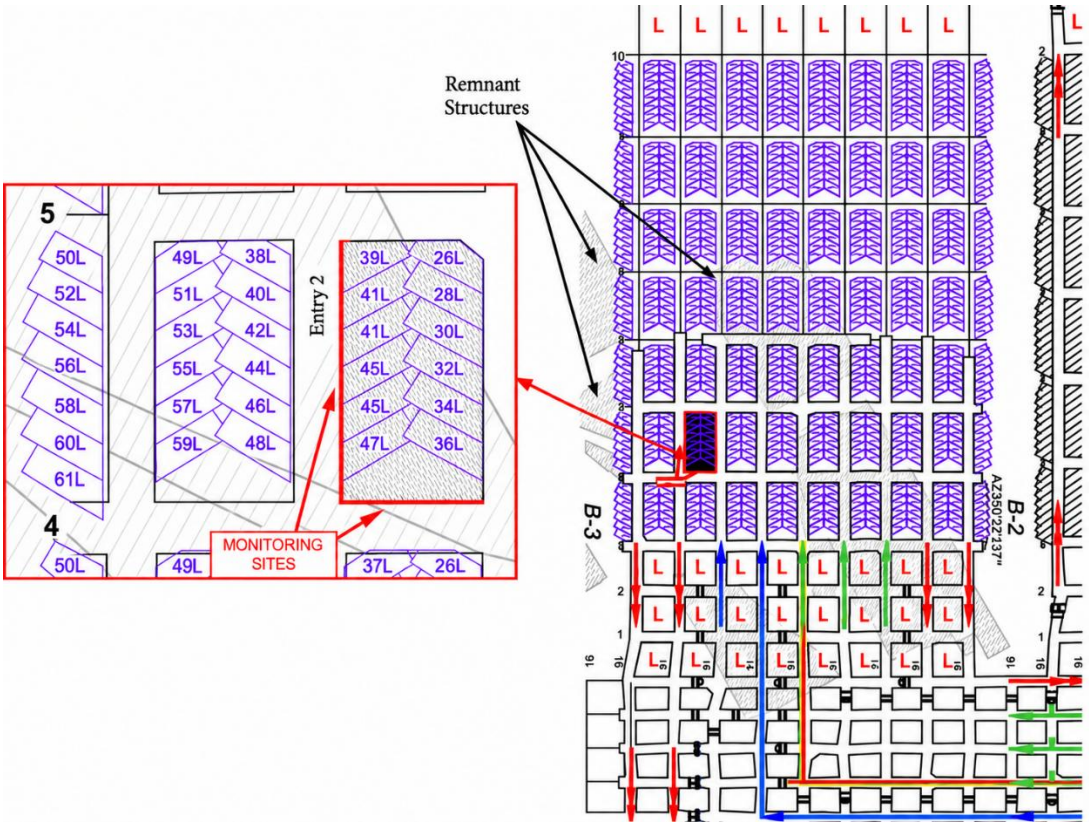


Figure 6: Study panel (B-2) and location of the study site, located between crosscuts No. 4 and 5.

The ACPS-estimated critical interburden thickness is 110 ft during the development stage and 197 ft during the pillar retreat stage (Mark & Agioutantis, 2019). Because the actual interburden thickness at the study site is approximately 180 ft, it exceeds the development-stage critical thickness but is below the pillar-retreat critical thickness. Therefore, slight multiple-seam interaction was expected during the retreat stage.

Instrument Layout Description

The instruments were installed in the pillar while the continuous miner was advancing one break inby the instrumented pillar during the development phase of the panel's mining schedule. Figure 7 illustrates a scaled layout of the instrumented pillar, showing the positions of roof extensometers

(RX), load cells (LC), borehole pressure cells (BPC), and multi-point borehole extensometers (MPBX). Table 1 provides a list of all instrumentation installed in the pillar for data collection.

Table 1: Summary of instrumentation used at the study site.

Instrumentation Type	Quantity	Location/Specification
Roof Extensometer 1	1	Anchored at 15 ft depth in the entry roof
Roof Extensometer 2	1	Anchored at 15 ft depth in the crosscut roof
Multi-Point Borehole Extensometer (MPBX) 1	1	Anchors located at 8 ft, 14 ft, 20 ft, and 30 ft depths in the entry rib
Multi-Point Borehole Extensometer (MPBX) 2	1	Anchors located at 6 ft, 12 ft, 18 ft, and 30 ft depths in the entry rib
Multi-Point Borehole Extensometer (MPBX) 3	1	Anchors located at 4 ft, 10 ft, 16 ft, and 30 ft depths in the entry rib
Multi-Point Borehole Extensometer (MPBX) 4	1	Anchors located at 8 ft, 14 ft, 20 ft, and 30 ft depths in the crosscut rib
Multi-Point Borehole Extensometer (MPBX) 5	1	Anchors located at 6 ft, 12 ft, 18 ft, and 30 ft depths in the crosscut rib
Multi-Point Borehole Extensometer (MPBX) 6	1	Anchors located at 4 ft, 10 ft, 16 ft, and 30 ft depths in the crosscut rib
Rib Bolt Load Cells (LC)	3	Mounted on No. 5, Grade 60, 5-ft length fully grouted rib bolts in the entry rib
Rib Bolt Load Cells (LC)	3	Mounted on No. 5, Grade 60, 5-ft length fully grouted rib bolts in the crosscut rib
Borehole Pressure Cells (BPC)	3	Located at 10 ft, 20 ft, and 30 ft depths in the entry side rib
Borehole Pressure Cells (BPC)	3	Located at 10 ft, 20 ft, and 30 ft depths in the crosscut side rib

Roof extensometers RX1 and RX2 were installed to monitor roof displacements in the middle of entry #2 and crosscut #4, respectively. The anchor point for each roof extensometer was positioned at a depth of 15 ft into the roof, which is approximately equal to the width of the entry at the study site. This depth was selected to ensure that the anchors would experience minimal induced stress from both the entry and the crosscut. Load cells (LC) were mounted on 5-ft-long, No. 5, Grade 60 rib bolts with a grout length of 60 in to measure the induced loads in the rib bolts at both the entry and the crosscut. LC-1, LC-2, and LC-3 were installed on the entry side (entry No. 2) of the instrumented pillar, while LC-4, LC-5, and LC-6 were installed on the crosscut side (crosscut No.

4) of the instrumented pillar. The Mine Instrumentation Data Acquisition System (MIDAS) used during the monitoring period was positioned one break outby the instrumented pillar to maximize data continuity and protect the system during retreat operations.

The initial plan also included attaching sensors at the pillar corners to monitor potential stress concentrations and deformation. However, the responsible mine engineer and experienced NIOSH technicians determined that this approach was not suitable, as corner installations would be highly susceptible to damage. This vulnerability could result in premature data loss and compromised sensor performance in the early stages of the retreat, limiting the effectiveness of the instrumentation in capturing the full range of responses. Furthermore, installing instrumentation in the pillar corner risked disturbing the corner and increasing local instability and associated hazards. Because of this constraint, pillar corner response data could not be collected during this monitoring study.

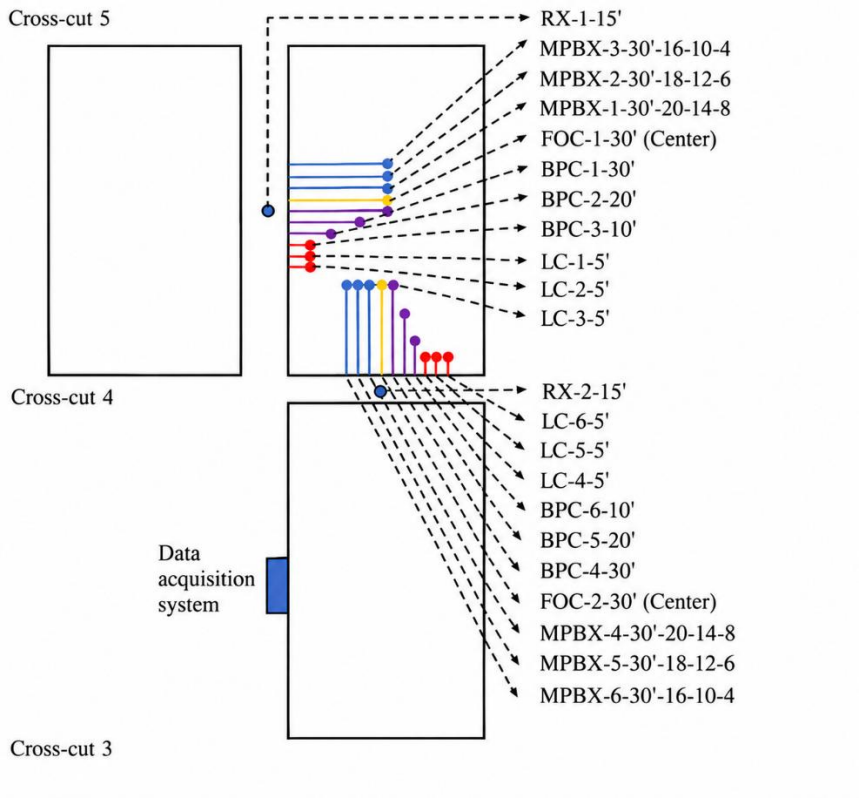


Figure 7: Detailed view of the instrumentation layout (LC = load cell, BPC = borehole pressure cell, RX = 4-point roof extensometer, MPBX = 4-point rib extensometer).

Field Observations Summary

The roof, floor, rib, and caving conditions from entry #1 to #9 were surveyed when the pillar line was one and two breaks inby the studied pillar. The roof caved well inby the pillar lines, and roof overhanging was observed at entries #1 and #9, resulting from the presence of barrier pillars. The good roof caving conditions limited stress transfer to the active mining zone. There were no signs of roof or floor deformation outby the active retreat pillar line. Rib conditions were generally good,

with little to no sloughing, except at the pillar being mined, where rib movement initiated at the coal-rock interface.

Before the initiation of retreat operations at the instrumented pillar, particular attention was given to roof caving conditions and rib behavior at neighboring pillars. A site visit was specifically scheduled to conduct a comprehensive assessment of roof caving conditions and equipment placement before retreating of the instrumented pillar began. The results of this survey are presented in Figure 8. Nine specific observation points, termed stations, were selected for this evaluation.

Station #1, situated at entry #1 between crosscuts #5 and #6, showed favorable roof caving conditions and formation of gob material. In addition to the good caving conditions, no signs of load transfer were observed, and the roof and floor conditions at the neighboring pillars were favorable.

Similar conditions and gob formation were observed at Station #2. In contrast, gob material was not observed at Station #3, and signs of stress transfer were observed in the neighboring pillars. Areas of roof overhang were also noted. Rib sloughing and surface chipping, particularly near the pillar corners, were observed in the neighboring pillars where stress concentrations were evident.

This visit coincided with the beginning of retreat operations at entry #4 and between crosscuts #5 and #6 on the same date. Consequently, mobile roof supports (MRS) were positioned one break ahead of Station #4 instead of wooden brakes due to ongoing retreat operations. During the assessment of Station #4, no caving was observed, although the roof exhibited signs of downward movement similar to the observations at Station #3. Although roof and floor conditions remained favorable, the unmined rib showed signs of damage and potential instability around the MRS. This observation illustrated the effect of abutment loading on stress concentration in the pillars during retreat operations and its associated influence on rib stability.

The subsequent assessment at Station #5, located one crosscut inby Stations #1, #2, and #3, also showed no caving conditions of gob formation, similar to Stations #3 and #4. While the roof had not caved and no gob had formed at these three stations, significant roof convergence was observed inby them. This was a strong indication that caving and gob formation were imminent, but this was not observed during the scheduled site visit.

The following assessment at Stations #6, #7, #8, and #9 showed good caving conditions with gob formation, similar to Stations #1 and #2. This gob formation released stress on the neighboring pillars, resulting in good rib conditions and no signs of stress transfer to pillars around these stations. This highlights the critical nature of good caving conditions and gob formation during the retreat stage of a room-and-pillar coal mining operation.

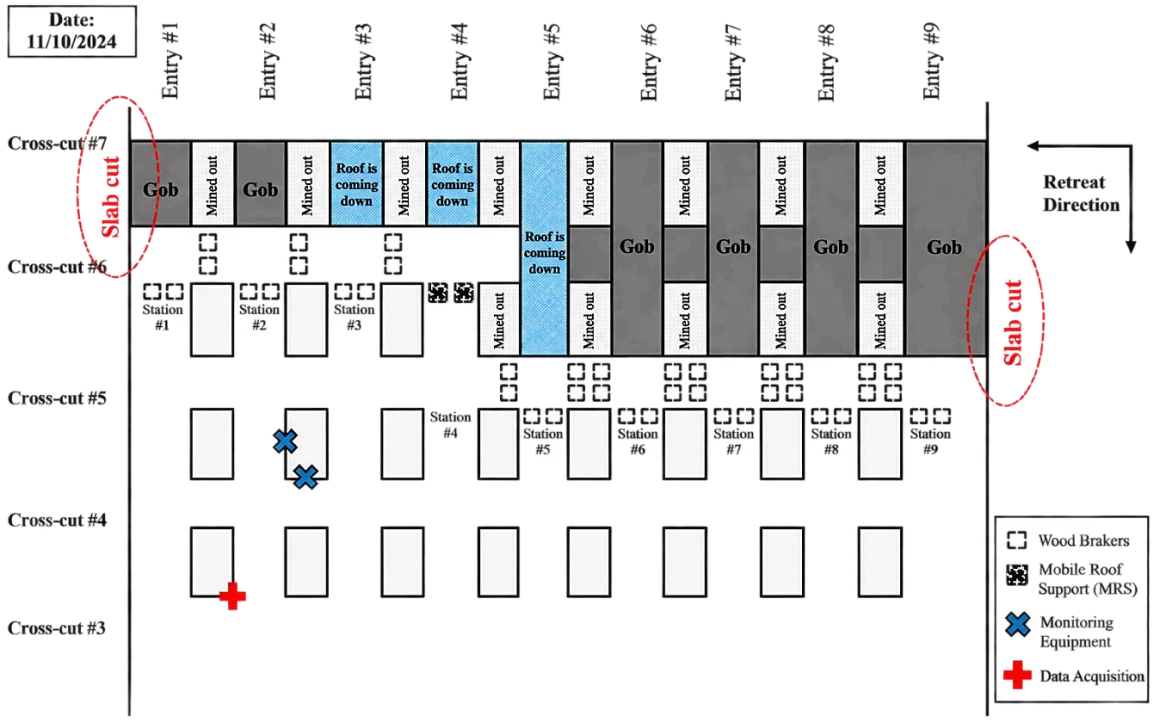


Figure 8: Locations of visual observation stations, retreat direction, and observed caving conditions.

Instrumentation Results Summary

The monitoring effort lasted 50 days, allowing for a comprehensive observation of the rib performance of the instrumented pillar under changing loading conditions. Although most of the recorded instrument data remained stable, reliable data could not be obtained from two MPBXs (MPBX-5 and MPBX-6) located in the crosscut and from both roof extensometers (RXs). No issues were identified in the RX connection cables; therefore, the unreliable readings were believed to result from the RX springs not being fully secured within the boreholes. Additionally, MPBX-5 and MPBX-6 were suspected to have malfunctioned because of wire damage caused by mining equipment.

Figure 9 illustrates the pillar retreat sequence and the retreat dates for the three breaks inby the instrumented pillar (designated as P7). The pillar retreat in the B-2 panel began at crosscut 10, located six breaks inby the instrumented pillar P7. In the study mine, the pillar retreat sequence advances from right to left, beginning with the pillar closest to the previously mined B-1 panel. The pillars in the same row as the instrumented pillar were labeled sequentially from P1 to P7 according to their retreat sequence. This labeling was used in the subsequent monitoring plots.

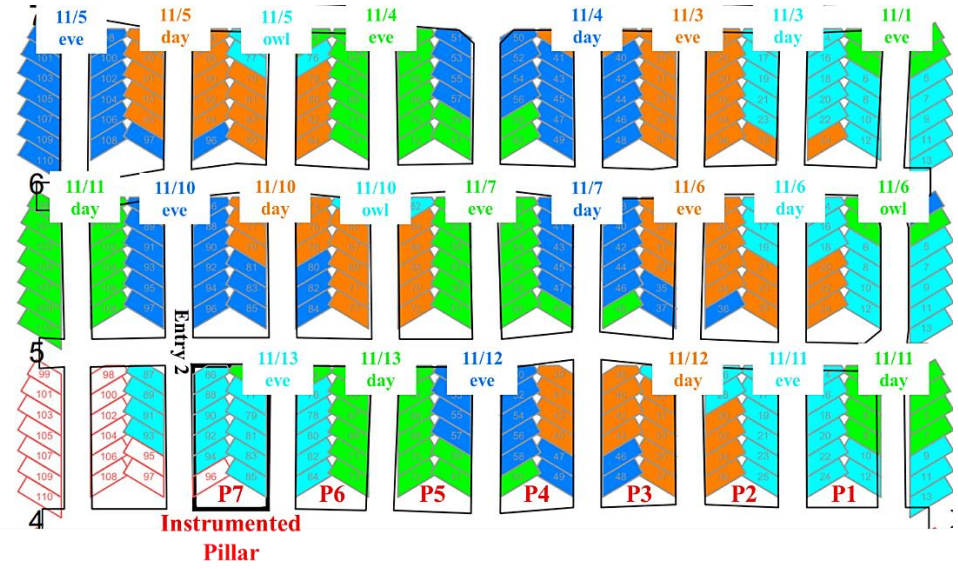


Figure 9: Pillar retreat sequence and the retreat dates.

Pressure Change in the Instrumented Pillar

Visual observations indicated that the rock parting in the coal pillar ribs remained intact during the retreat of the pillars, including small pillars (stumps) left in the gob area. This stability was attributed to the high strength of the shale, which was estimated at about 5,000 psi, along with the use of rib bolts to support the rock parting. As the roof converges, the rock parting presses against the coal seam in the coal pillar ribs. The pressure changes within the coal seam were monitored using BPCs, as illustrated in Figure 10 for the entire monitoring period and in Figure 11 for the period following the initiation of pillar retreat along the instrumented pillar line (starting from the P1 pillar retreat).

As seen in Figure 10, the pressure changes in the instrumented pillar remained below 100 psi for all sensors until November 4. This date approximately corresponded to the point when the retreating process reached a distance of two breaks from the instrumented pillar. Furthermore, Figure 11 shows that the sudden increase in pressure change began with the retreat of the neighboring pillar, P6.

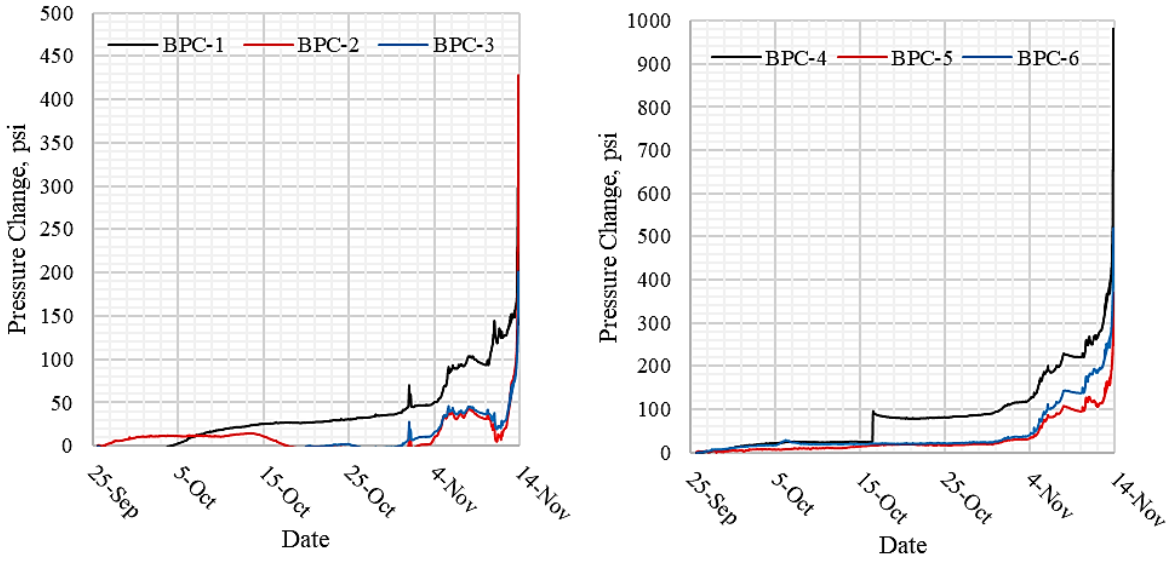
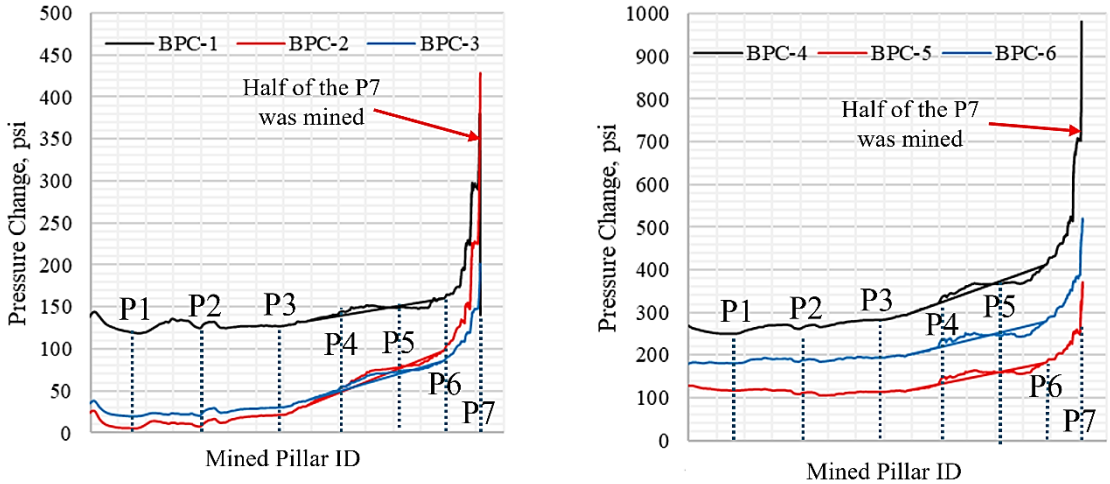


Figure 10: Pressure changes in the BPCs for the entry (left) and crosscut sides (right) for the entire monitoring period.

The pressures recorded by the BPCs on the crosscut side were greater than those recorded on the entry side, which was attributed to the retreat direction. When half of the instrumented pillar was mined, the average pressure change at the crosscut was approximately 500 psi, nearly twice that at the entry side.

Figure 11: Pressure changes in the BPCs for the entry (left) and crosscut sides (right) following the initiation of pillar retreat along the instrumented pillar break.



Load Change in the Instrumented Pillar

Figure 12 shows the changes in load on the instrumented rib bolts installed on both the entry side and the crosscut side of the instrumented pillar. As observed in the results from the BPCs, the load

cells mounted on the rib bolts continued to provide load measurements until half of the instrumented pillar was mined. Similar to the BPC data, when the retreating process reached a distance of two breaks from the instrumented pillar around November 4th, the applied load on the rib bolts began to increase. Before this point, a small load was induced in the ungrouted length of the rib bolts due to rib dilation. This load ranged from 100 to 500 lb, which represented approximately 2% of the yield capacity of the rib bolts. After this date, rib sloughing was also observed in the instrumented and neighboring pillars. Figure 12 also shows that the instrumented rib bolts sustained a load of up to 5,000 lb, which is approximately 25% of their yield capacity, during the retreat of the instrumented pillar.

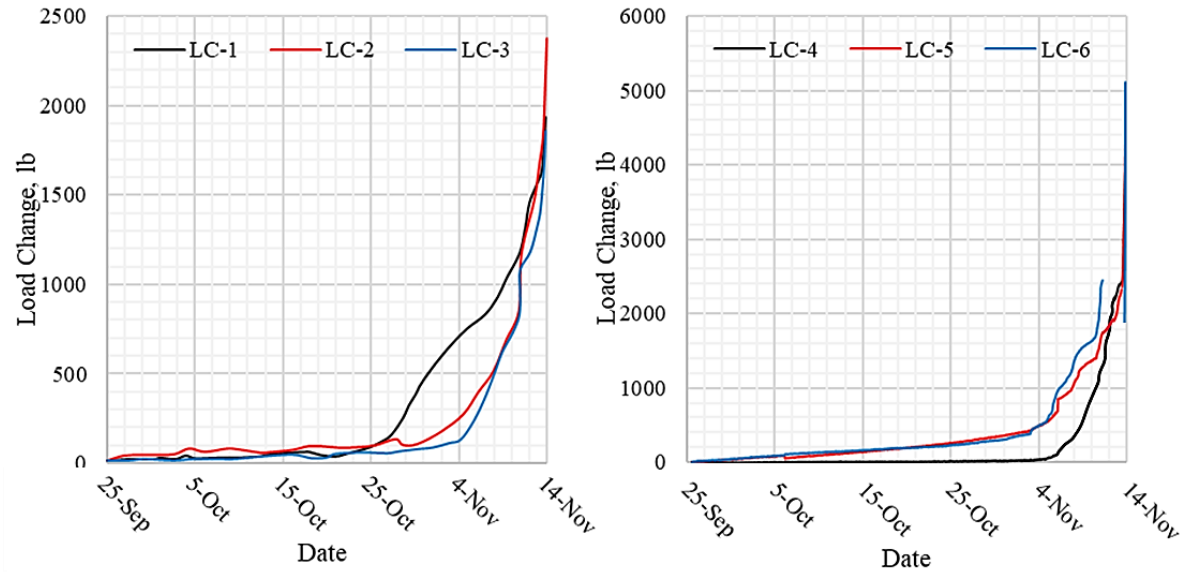


Figure 12: Changes in rib bolt load for the entry (left) and crosscut (right) sides.

Rib Displacement

Reliable data could not be obtained from two of the MPBXs installed on the crosscut side. The MPBXs recorded negligible displacement readings until the retreat line reached a distance of two breaks from the instrumented pillar (November 4; See Figure 13). The deformation readings, which began to increase after this point, increased approximately fourfold when the retreat reached one break away. The next notable increase in the displacement rate was observed when retreating began at the instrumented pillar. As expected, higher displacements were observed at the measurement point closest to the rib face in all the MPBXs from which data were obtained. The maximum rib displacement was 0.1 inches and occurred when the pillar adjacent to the instrumented pillar was mined out. This small rib displacement was not anticipated to cause significant fractures in the rib, which was confirmed by field observations. The relatively small displacement was attributed to the high strength of the coal and rock partings.

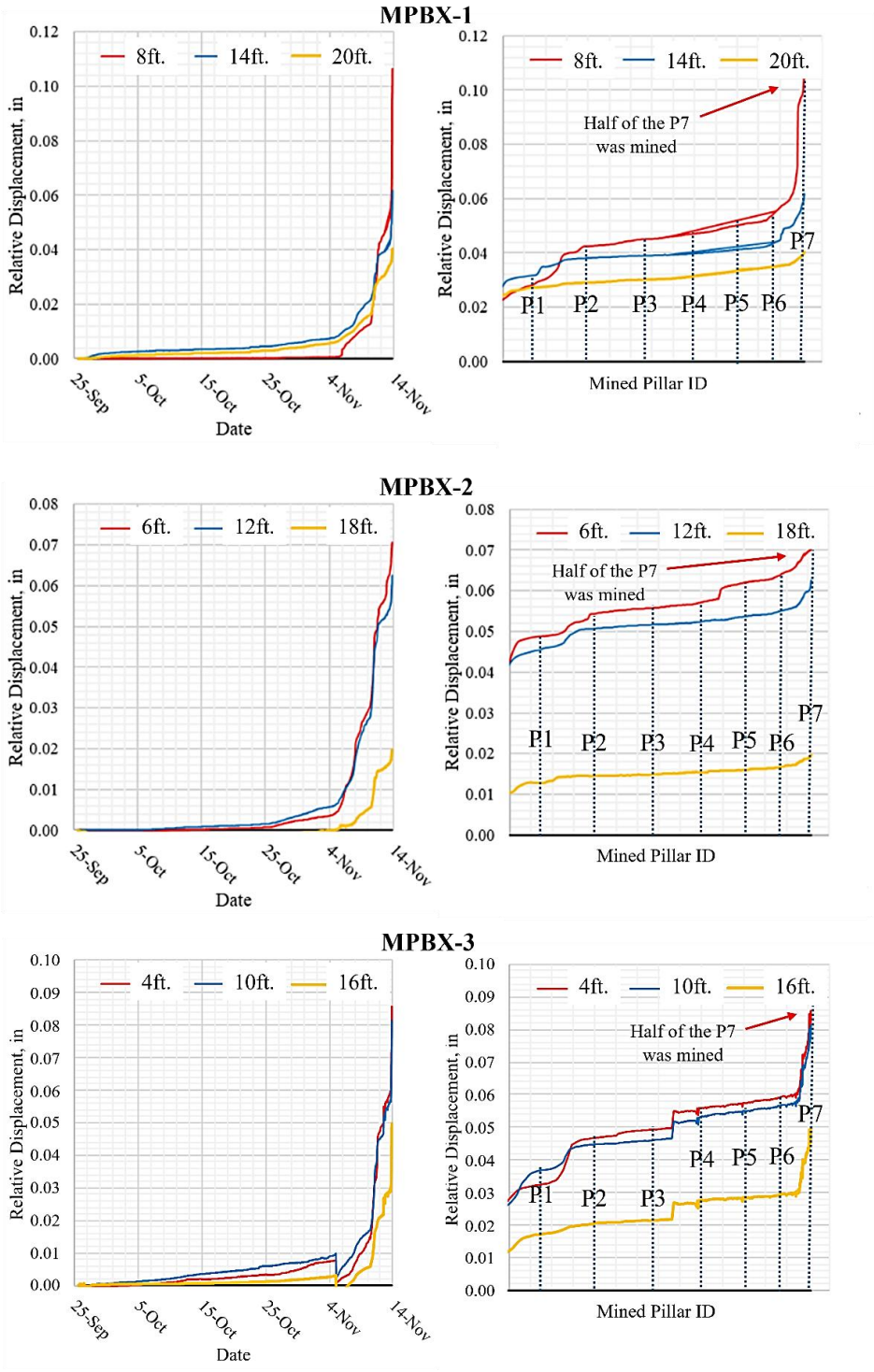


Figure 13: Recorded relative rib displacements at the entry side of the instrumented pillar.

It should be noted that the MPBX data do not directly represent rib sloughage at the rib surface. For MPBX-4, the measurement point closest to the rib face was located at a depth of 8 ft. At the point where instrumentation was discontinued, rib sloughage reaching up to 1.5 ft was observed at

the corners of the instrumented pillar, whereas at the mid-span of the pillar on the entry side, rib sloughage was below 1 ft. The only MPBX data obtained from the crosscut side were significantly lower than the entry-side data, contrary to expectations and field observations (Figure 14). Considering the observed instrumentation problems with MPBX-5 and MPBX-6, combined with the significantly low readings from MPBX-4, the crosscut-side MPBX data were excluded from further consideration, as instrument damage was suspected for MPBX-4 as well.

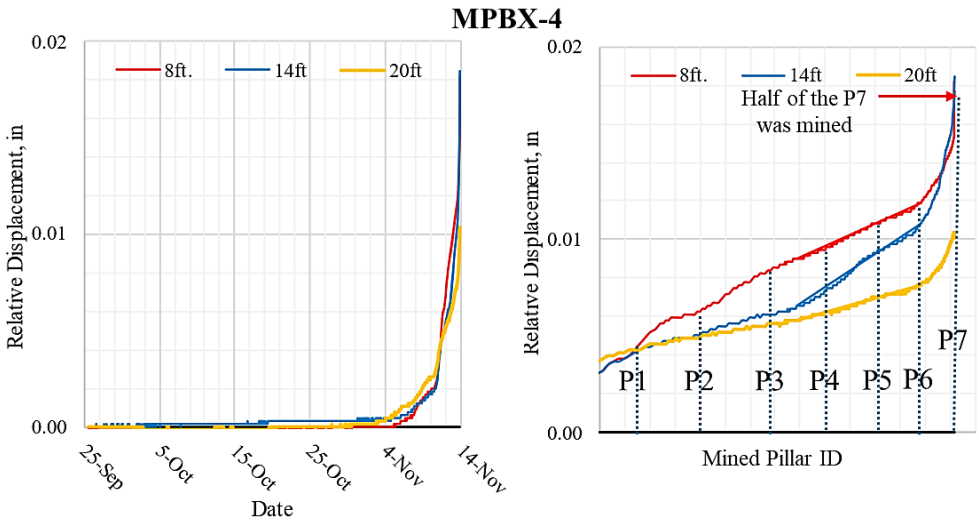


Figure 14: Recorded relative rib displacements on the crosscut side of the instrumented pillar.

The combination of field observations during the retreating process and the response measured in the instrumented pillar provided insight into coal pillar rib behavior, particularly as abutment loading developed during pillar retreating. The instrumented pillar began taking additional load when the retreat line was approximately two breaks inby, indicating the onset of abutment-loading effects that can adversely affect coal rib stability. Across stress, bolt loading, and rib displacement responses, a consistent trend was observed: abutment loading began to affect the instrumented pillar when the retreat line was two breaks inby and continued to increase as the retreat line approached. Retreating the neighboring pillar was followed by an immediate increase in loading on the instrumented pillar, which continued until the instrumented pillar was subsequently retreated. In cases of poor caving and gob formation during retreat, this behavior could be further intensified because of reduced stress relief associated with delayed roof caving.

3.2. Objective 2: Quantify the Effects of MSI and Abutment Loading on Coal Rib Stability and Evaluate Rib-Corner Stability

3.2.1. Task #3. Numerical Model Development

The focus of this task was to develop the numerical modeling methodology used to quantify the effects of MSI and abutment loading on coal rib stability, and to evaluate rib-corner stability and potential support configurations. To effectively model coal ribs and their mechanical behavior, the three-dimensional distinct element code (3DEC), developed by the Itasca Consulting Group, was

used. This modeling software's ability to represent a rock mass as a system of deformable blocks with explicit contact interaction (Itasca Consulting Group, 2021) is critical to accurately capture the complex interactions between stress-driven and kinematic mechanisms observed in coal ribs (Guner, Sherizadeh, et al., 2023; Mohamed et al., 2023).

2D Mid-Rib Numerical Models

The 2D numerical models used for the MSI and abutment-loading analyses were initially developed and calibrated as part of our research team's previously completed Alpha Foundation projects (Sherizadeh, 2023; Sherizadeh et al., 2024). Similarly, as part of this previous work, direct comparisons between the developed 2D numerical models and specific case data were made to further strengthen parametric analysis. To evaluate MSI and abutment loading effects on RibFOS, 2D plane-strain models were used to represent the mid-span of a coal rib under development, MSI, and abutment loading conditions. Figure 15 illustrates the geometry, boundary conditions, and explicit joints of a representative 2D model used for the numerical analysis of MSI and abutment loading conditions.

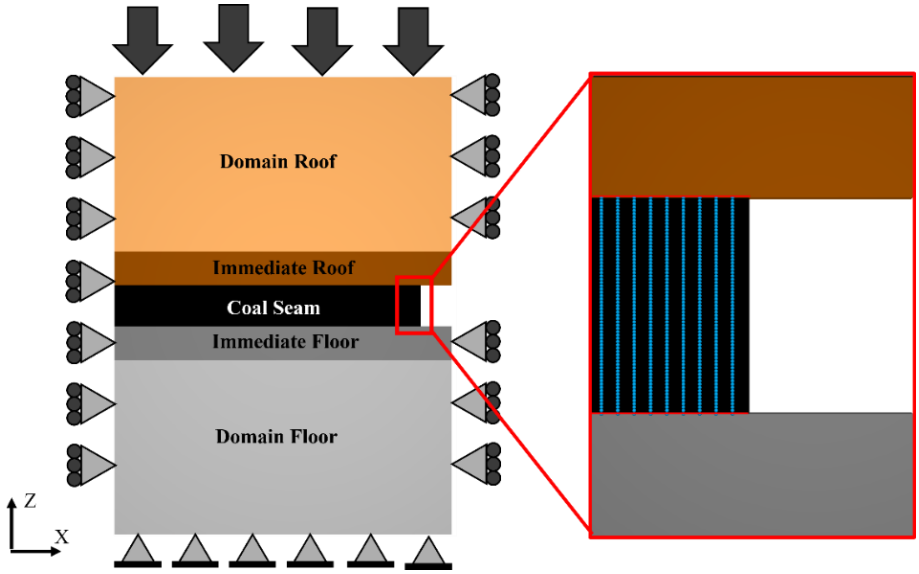


Figure 15: Model geometry and boundary conditions. The zoomed-in view illustrates face cleats (blue) and roof/floor contacts (red).

The 2D models were fixed at the bottom boundary, and the sides were fixed in the X direction. Out-of-plane displacements were fixed to enforce the plane-strain 2D condition used in the parametric models. The upper boundary was subjected to the vertical stress corresponding to the overburden depth for each parametric case. The maximum horizontal stress was oriented parallel to the entry to represent the worst-case loading condition for the entry ribs and to maintain consistency with previous modeling efforts. The in-situ horizontal stresses in the coal units were determined using methods developed by Liu et al. (2016) (Eqs. 3, 4, and 5). The horizontal stresses in the rock units were determined using equations recommended by Esterhuizen (2017), as applied by Mohamed et al. (2019) (Eqs. 3, 6, and 7).

$$\sigma_v = \gamma \times Z \quad (3)$$

$$\sigma_{Hc} = 1.174 + 0.024 \times Z_c \quad (4)$$

$$\sigma_{hc} = 0.018 \times Z_c - 1.475 \quad (5)$$

$$\sigma_{Hr} = 0.313 + 0.027 \times Z_r + 0.000278 \times E_r \quad (6)$$

$$\sigma_{hr} = 0.65 \times \sigma_{Hr} \quad (7)$$

σ_v represents the vertical stress for coal units and rock layers, and γ is the specific weight of the geologic layers in MN/m^3. σ_{Hc} and σ_{hc} are the maximum and minimum horizontal stresses of the coal units in MPa, respectively, and σ_{Hr} and σ_{hr} are the maximum and minimum horizontal stresses of the rock units in MPa, respectively. Z_c and Z_r are the depths of the coal and rock units in meters, respectively, and E_r is the Young's modulus of the rock layers in MPa.

Consistent with our previous work and to represent the worst-case scenario, face cleats were oriented parallel to the entry with butt cleats oriented perpendicular to the entry. Given that the models were 2D, the butt cleats were not explicitly modeled. This configuration was consistent with field observations, where the face cleat system was the dominant rib structure for the selected cleat orientation, indicating that the butt cleats did not have a significant impact on entry mid-rib behavior compared to the face cleats. The cleat properties used in the numerical models were consistent with those reported in our previous Alpha Foundation project report (Sherizadeh, 2023).

A graded mesh was used in the models to maximize computational efficiency while maintaining sufficient resolution in the immediate rib region. The mesh sizes used in the 2D models were 5 cm (2 in) in the fine region encompassing the immediate rib region, 12.5 cm (4.9 in) in the intermediate region behind the fine region and extending into the immediate roof and floor, and 32 cm (12.6 in) outside of the intermediate mesh zone.

The coal unit(s) were simulated using the coal mass constitutive model developed by NIOSH researchers and adapted for use in 3DEC as part of our past research efforts (Mohamed et al., 2018; Sherizadeh, 2023). Rock partings, the immediate roof/floor, and the domain roof/floor were modeled using the Mohr-Coulomb constitutive model to maintain consistency with the modeling parameters used in our past coal rib research efforts (Sherizadeh, 2023; Sherizadeh et al., 2024). For the 2D numerical models, the calibrated properties from our previous coal rib research were directly used to maintain consistency in the development of the coal rib control system.

For all models, the in-situ stresses were first initialized using Equations (3) – (7), and the models were solved to equilibrium. After reaching equilibrium, the reaction forces at the excavation boundary were stored, and the excavation region elements were deleted. The stored reaction forces were then reapplied to the excavation boundary to minimize numerical shock associated with excavation. The reaction forces were then reduced nonlinearly as a function of the step number divided by 1,000 to simulate the gradual unloading and softening response of the coal rib. After the reaction forces were fully reduced and removed, the models were solved to equilibrium again to ensure that no significant out-of-balance forces remained and that the rib response was fully

captured. These steps were repeated for all modeling cases and were considered representative of coal rib response under development conditions.

To analyze rib stability in the parametric studies, a displacement-based stability criterion was used to determine stable and unstable rib conditions and RibFOS values. The modeled rib was classified as unstable when displacement exceeding 1 cm (0.4 in) was observed at a depth of 25 cm (9.8 in) or greater from the rib surface. The stability criterion was developed based on extensive field observations and numerical modeling outputs from coal rib stability analyses (Guner, Sherizadeh, et al., 2023).

For each model scenario, the strength reduction method was used to evaluate rib stability and determine its RibFOS. Specifically, the coal mass scale parameter (CMS) was reduced by the reduction factor to simulate strength reduction in the numerical material matrix. Similarly, the joint peak and residual cohesion and tension values were reduced by the same factor. This modeling methodology was consistent with the steps followed in our previously completed coal rib stability research (Sherizadeh, 2023; Sherizadeh et al., 2024) and was utilized to maintain numerical modeling and synthetic data consistency during the coal rib control system's development.

For the parametric analysis of MSI effects and abutment loading conditions, the following mining and geological conditions were explored: overburden depth, rib height, coal lithotype, bedding plane condition, the presence of a rock parting in the rib, and rock parting strength. The specific parameter levels explored in the parametric studies are presented in Table 2.

Table 2: Studied mining and geological parameters and their ranges.

Parameter	Range
Overburden Depth (ft)	300 to 1,050
Rib Height (ft)	5 to 11
Coal UCS (PSI)	BC[1] - 1,250; BBC[2] - 2,857; DC[3] - 5,075
Rock Parting UCS (PSI)	Moderate: 7,397; Weak: 3,481
Rock Parting Thickness (ft)	1 to 4
Bedding Plane Condition	Strong; Weak

1 – Bright Coal; 2 – Banded-Bright Coal; 3 – Dull Coal

Using Table 2, combinations of mining and geological parameter levels were generated to establish a parametric study model scenario set used for analyzing the effect of MSI and abutment loading on coal rib stability (represented by rib factor of safety or RibFOS). Before moving forward with the parametric studies, it was first necessary to curate the full parametric design space to exclude parameter combinations that are unrealistic and ensure that realistic coal rib scenarios were used to inform the developed MSI and abutment loading relationships with RibFOS. For example, it is unlikely that a coal rib would be composed of DC coal at an overburden depth of 300 ft. After reducing the parametric design space, 58 numerical model scenarios were selected to evaluate the effect of MSI and abutment loading conditions on RibFOS to facilitate expanding the capabilities of the coal rib control system and RSRT application.

3D Rib-Corner Numerical Models

Modeling the coal pillar rib corners required extending the 2D modeling methodology used for the MSI and abutment loading models to 3D to represent the pillar corner and its response. Because adding the third dimension significantly increased computational complexity, it was not feasible to model the full pillar geometry with a sufficiently fine mesh in the corner region. To resolve this, the pillar geometry was modeled with two symmetry planes to represent a quarter pillar and focus on a single corner. For the corner models, the model dimensions were 15 m (49.2 ft) along the entry direction (Y direction) and 10 m (32.8 ft) along the crosscut direction (X direction). These dimensions were selected to represent the approximate pillar geometry observed during the instrumentation study.

The 3D corner models retained the constitutive models and in-situ stress initialization described for the 2D mid-rib models. As mentioned previously in Section 3.1.2, instrumentation could not be installed at the pillar corners; therefore, direct measurements of rib-corner response were not available for calibrating the 3D corner models. To address this constraint, the numerical properties used in the calibrated 2D models were directly used in the 3D corner models to ensure cross-model consistency.

Similar to the 2D mid-rib models, the 3D corner models used a graded mesh across three regions to maximize mesh resolution in the immediate corner region. The fine mesh region, with an element size of 5 cm (2 in), was located within a 1.5 m (4.9 ft) by 1.5 m (4.9 ft) area extending from the corner edge and extended through the full rib height. The intermediate mesh zone, with an element size of 12.5 cm (4.9 in), covered the entire seam region outside of the fine mesh zone at the corner. The immediate roof and floor layers used an element size of 25 cm (9.8 in) to grade out from the seam region to the remaining model domain. The remaining region outside of the immediate roof and floor did not have an element size assigned to minimize the number of elements used outside of the model's analysis region and reduce computational complexity. Because the corner models were extended to 3D, butt cleats were explicitly included in the models along with the face cleats and other structural joints. The cleat spacing was consistent between the 2D and 3D models, with a spacing of 25 cm (9.8 in), consistent with the modeling approaches used

in our previous two Alpha Foundation research projects. Figure 16 illustrates a representative 3D corner model.

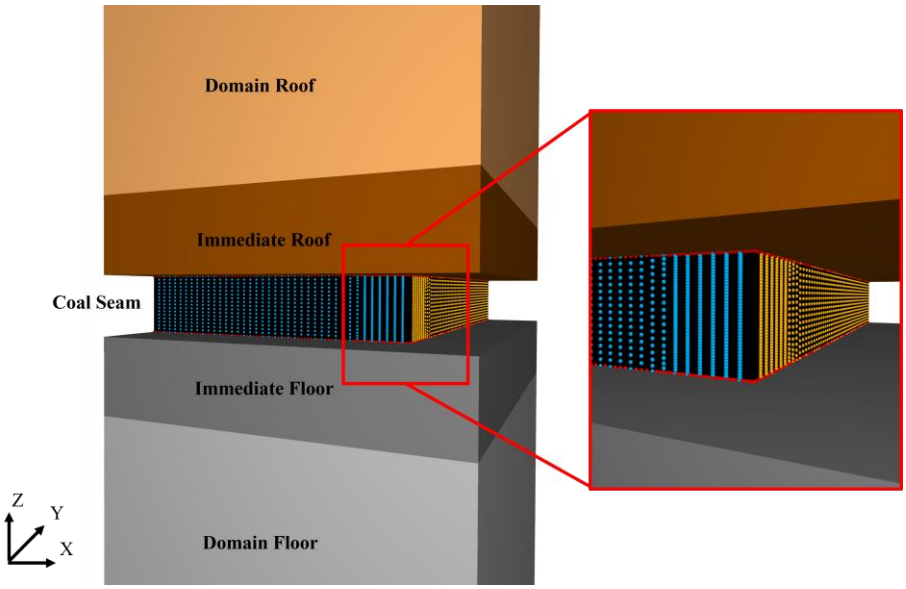


Figure 16: 3D corner model geometry and primary regions. The zoomed-in view illustrates face cleats (blue), butt cleats (yellow), and roof/floor contacts (red).

The 3D corner model excavations were split into two stages to reflect excavation staging observed during development at active coal mines. The entry excavation used the reaction-force storage, nonlinear unloading, and equilibrium procedures described for the 2D mid-rib models. Once the entry excavation stage converged, the same procedure was repeated for the crosscut excavation to evaluate the corner response under the defined mining and geological conditions.

RibFOS was not calculated for the 3D corner models. The displacement-based criterion described for the 2D models was used to define the mobilized corner zone, and its volume was used to compare unsupported and supported corner responses. The 2D development RibFOS values were used to select the corner-model scenarios. The scenario selection and corner-support comparisons are described in Section 3.2.2.

3.2.2. Task #4. Quantification of MSI and Abutment Loading Effects on RibFOS and Exploration of Rib-Corner Stability and Support Configurations

Effect of MSI on Coal Rib Stability

The first parametric study conducted as part of the research efforts focused on evaluating the effects of MSI on coal rib stability and establishing a relationship between MSI-induced vertical stress increases and RibFOS. Past research has shown that MSI can increase the vertical stress acting on a coal pillar (Mark et al., 2007a, 2007b). This research was further advanced by NIOSH researchers through development of the Analysis of Multiple Seam Stability (AMSS) methodology to evaluate vertical stress increases due to MSI effects, identify critical interburden thickness requirements for coal mine workings, and establish coal pillar safety factors that account for MSI effects on pillar stability (Mark et al., 2007a). Furthermore, the capabilities of AMSS and other

NIOSH coal pillar design methods were incorporated into the Analysis of Coal Pillar Stability (ACPS) software package to enhance coal pillar stability analysis and coal mine design (Mark & Agioutantis, 2019). Critically, ACPS focuses on coal pillar stability and does not directly evaluate the effects of MSI on coal rib stability. Therefore, this study used the MSI-induced vertical stress increase obtained from ACPS to establish a quantitative relationship between MSI and coal rib RibFOS.

Figure 17 provides an example output from the ACPS software package where two critical values are estimated: single-seam development stress and multiple-seam stress. The multiple-seam stress estimate provided by this software indicates the additional vertical stress caused by MSI effects, and the single-seam development stress provides an estimate of the initial vertical stress caused by the overburden depth without accounting for MSI effects. These two values can be used to determine a percentage increase in vertical stress, which is 62.1% for the example shown in Figure 17. Following this process, the parametric study evaluated vertical stress increases of 10%, 30%, 50%, 70%, and 90% to represent increasing MSI effects. For each of the 58 parametric model scenarios selected for this study, the model was solved under development conditions to determine a baseline RibFOS value using the strength reduction method. After establishing this baseline RibFOS value, the model was then solved for each of the vertical stress increase levels representing increasing MSI intensity. This resulted in almost 300 simulations and provided a sizable database for constructing the relationship between RibFOS and MSI effects. Comparing the development RibFOS with the MSI RibFOS across all scenarios provided direct multipliers representing the reduction in rib stability as MSI effects increase in intensity.

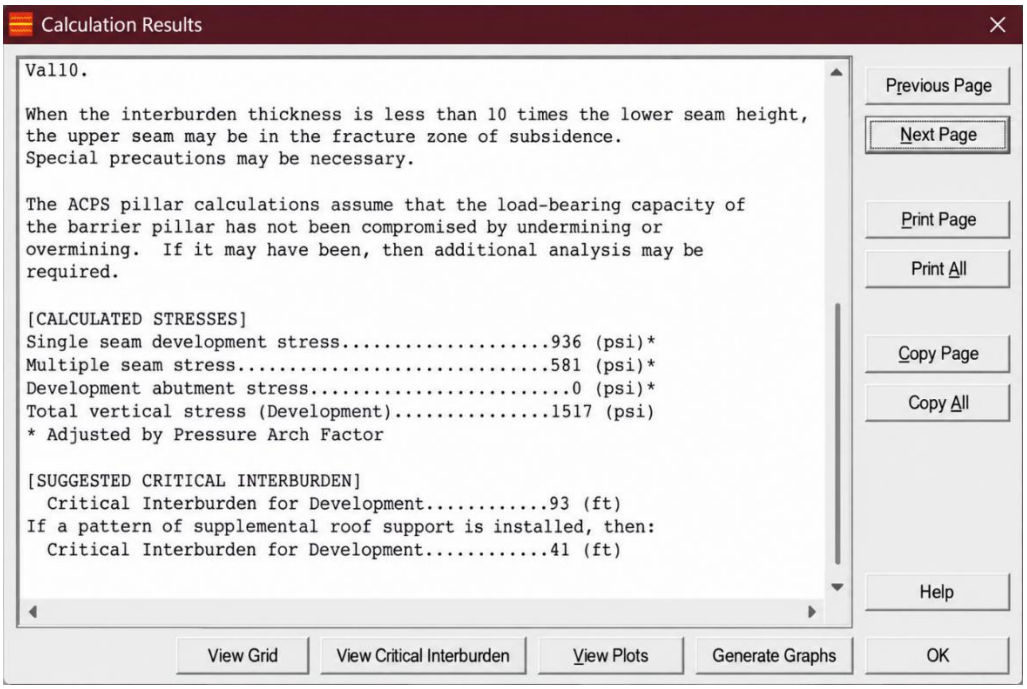


Figure 17: Example output from the ACPS software package providing MSI vertical stress and single seam vertical stress estimates based on an extensive case history database.

Figure 18 presents the relationship between MSI RibFOS and development RibFOS for single-solid coal rib configurations. Across the five vertical stress increase levels, the fitted regression equations show a consistent reduction in RibFOS as the MSI-induced vertical stress increase grows.

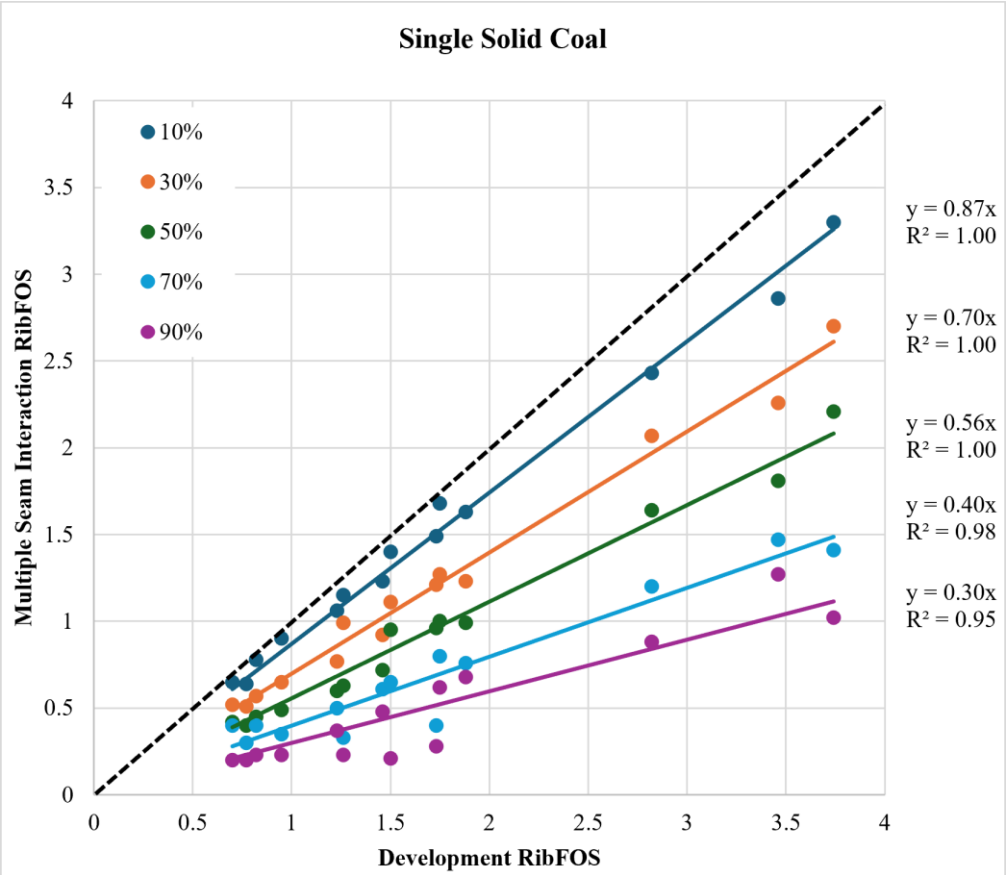


Figure 18: MSI RibFOS vs. Development RibFOS for single-solid coal rib configurations at each percent vertical stress increase level.

Figure 19 presents the same relationship for coal rib configurations containing a rock parting. Although greater variability is observed in this group, the same general trend between increasing vertical stress and decreasing RibFOS is maintained.

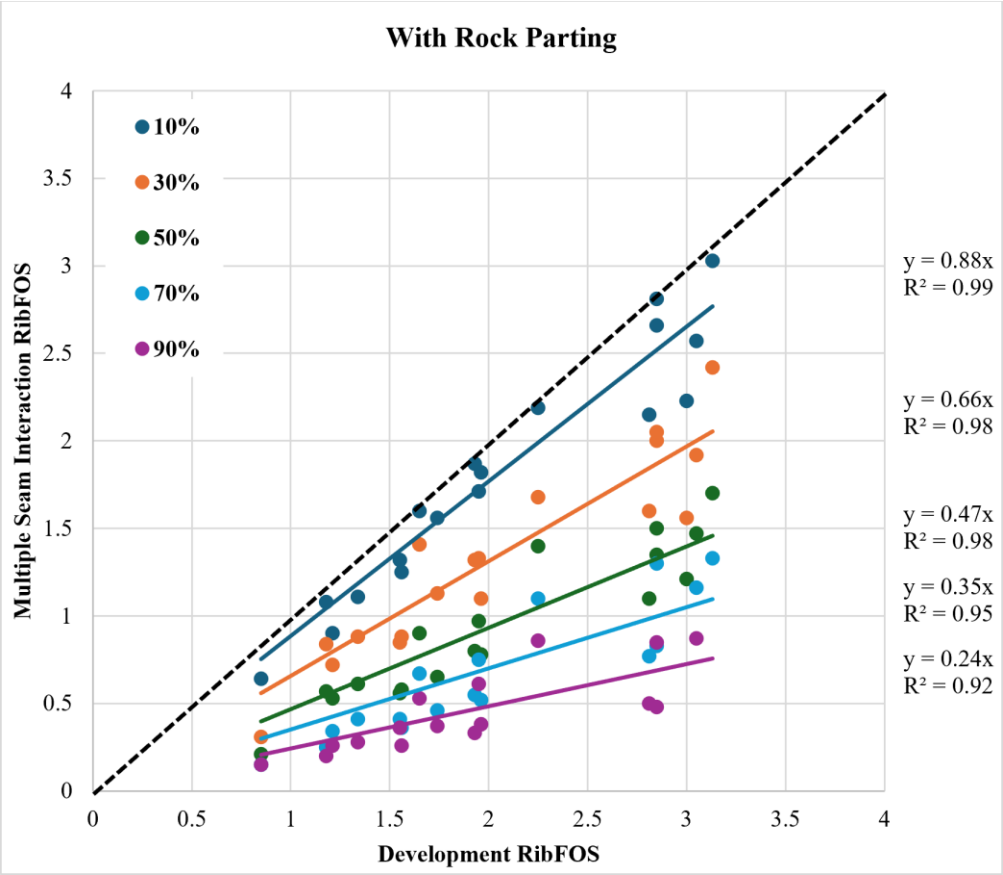


Figure 19: MSI RibFOS vs. Development RibFOS for coal rib configurations with a rock parting at each percent vertical stress increase level.

The final group of MSI models evaluated coal ribs with weak bedding planes between rib units (Figure 20). Similar to the other two sub-groups, the relationship between MSI RibFOS and development RibFOS remains consistent across the evaluated vertical stress increase levels.

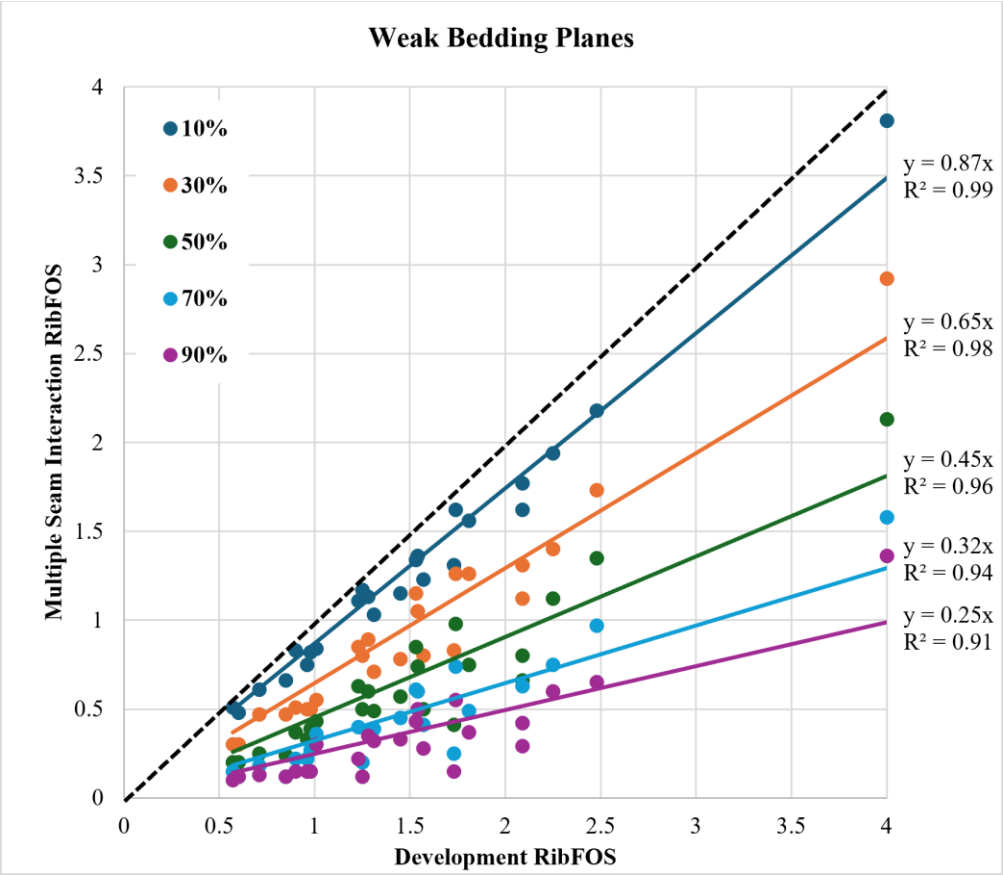


Figure 20: MSI RibFOS vs. Development RibFOS for coal rib configurations with weak bedding planes between rib units at each percent vertical stress increase level.

Since the trends in percent vertical stress increase were consistent across the three sub-groups, the results were combined to evaluate a generalized relationship between development RibFOS and MSI RibFOS. Figure 21 presents the pooled results for all coal rib configurations.

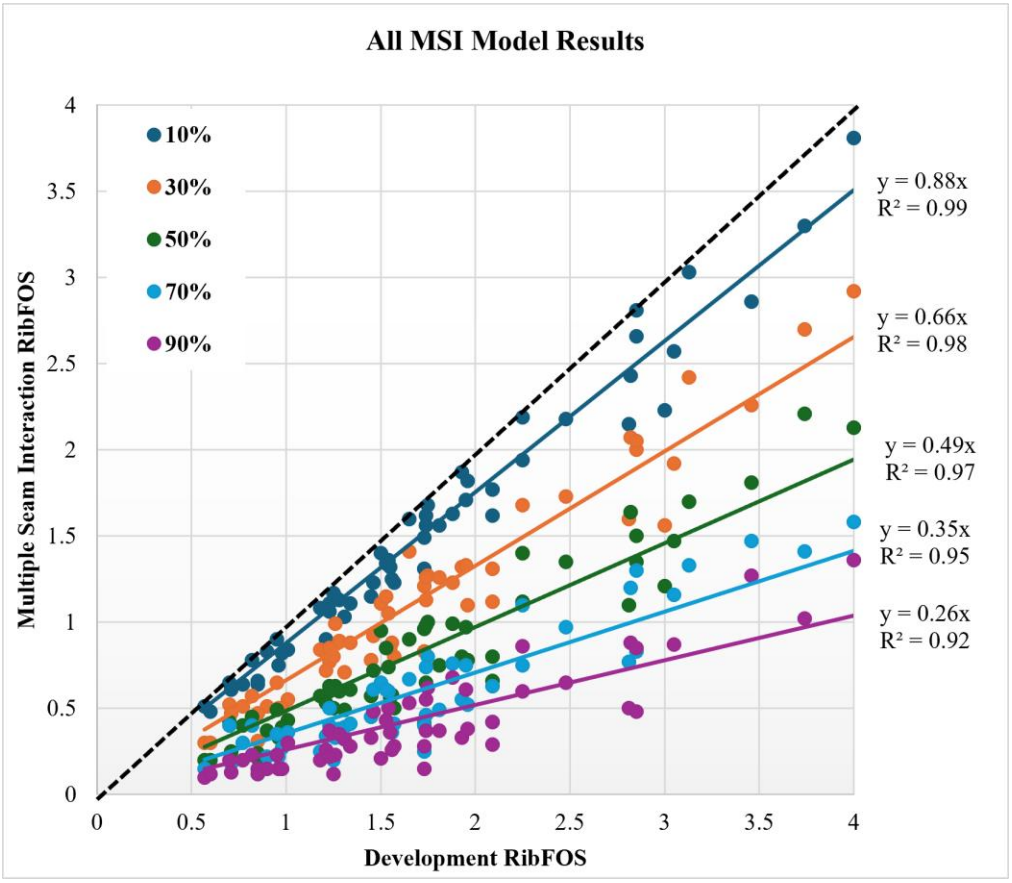


Figure 21: MSI RibFOS vs. Development RibFOS for all coal rib configurations at each percent vertical stress increase level.

Comparing the results of evaluating all sub-groups together, the pooled data show greater variability than the individual sub-group relationships. However, based on the coefficients of determination shown in Figure 21, the variability was sufficiently low to support development of generalized MSI RibFOS multipliers across the modeled rib configurations. These relationships provide generalized multipliers at each of the percent vertical stress increase levels evaluated during this stage of the research project. It is important to clarify that the multipliers defined from the regression equations in Figure 21 are only applicable at the specified percent vertical stress increase levels. To handle cases where the percent vertical stress increase falls between the explicit values outlined above, a final relationship was developed to connect the percent vertical stress increase value with the development RibFOS reduction multiplier. This relationship is presented in Figure 22.

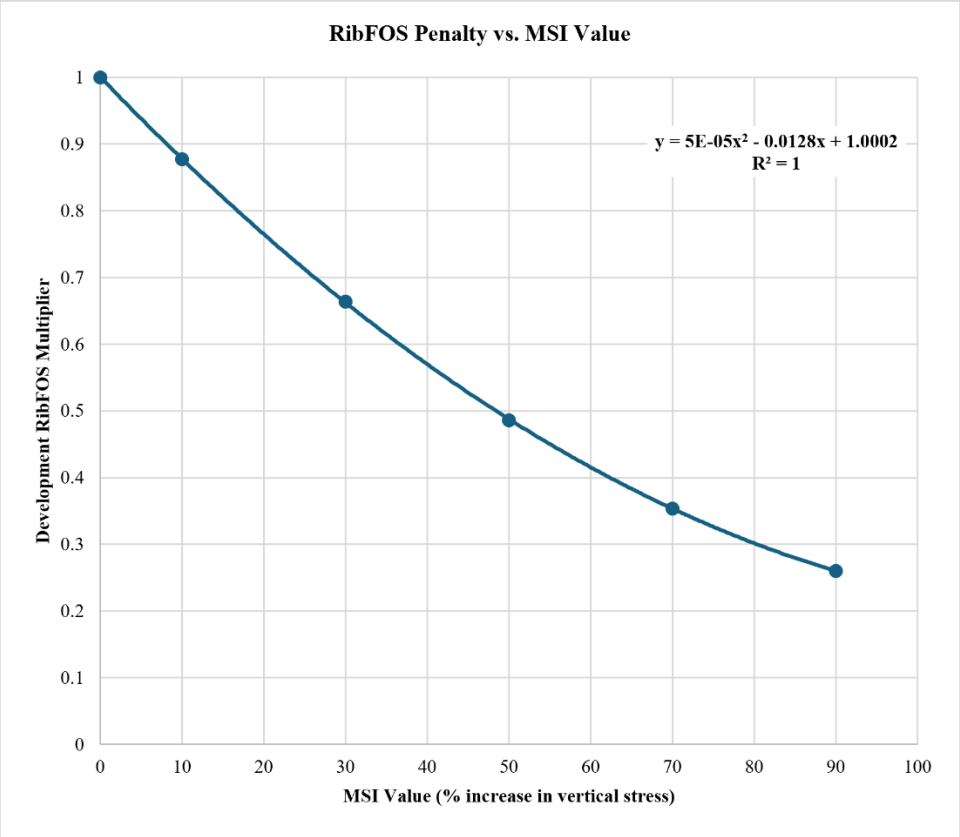


Figure 22: Development RibFOS multiplier vs. percent vertical stress increase determined from the ACPS software.

Figure 22 presents the generalized RibFOS multipliers obtained from the pooled numerical modeling results as a function of percent vertical stress increase. The high coefficient of determination of the fitted regression equation reflects the agreement between the developed relationship and the pooled multiplier values. This relationship provides a direct link between the MSI-induced vertical stress increase obtained from ACPS and the RibFOS adjustment used in the coal rib control system and RSRT. Equation 8 provides this relationship based on the pooled dataset of the modeled rib configurations.

$$RibFOS\ Multiplier = 5 \times 10^{-5} \times \sigma_{\%MSI}{}^{2} - 0.0128 \times \sigma_{\%MSI} + 1.0002 \quad (8)$$

Where $\sigma_{\%MSI}$ represents the increase in vertical stress as a percentage determined from ACPS outputs. Using Equation 8, the effective reduction multiplier for a percent increase in vertical stress due to MSI effects can be estimated and used to evaluate RibFOS in the RSRT application.

An important constraint of Equation 8 is the range of MSI-induced vertical stress increases evaluated in this study. The parametric study explicitly evaluated vertical stress increases from 10% to 90%. Mathematical extrapolation of the fitted quadratic beyond this range results in a minimum RibFOS multiplier of 0.181 at a vertical stress increase of approximately 128%, after which the equation begins to predict an increasing multiplier. Because this behavior occurs outside

the range evaluated in the numerical study, it should not be interpreted as a validated rib response. Therefore, Equation 8 should be applied within the evaluated 10% to 90% vertical stress increase range. Cases exceeding this range should be evaluated on a case-specific basis until additional numerical analyses are available to extend the relationship.

Effect of Abutment Loading on Coal Rib Stability

The second parametric study conducted as part of this research focused on quantifying the effects of side and face abutment loading on coal rib stability. The 58 parametric model scenarios curated from the full parametric design space were used to simulate development, side, and face abutment loading conditions for various coal rib configurations, resulting in 174 numerical simulations. Although the 2D rib models had been calibrated and validated as part of a previous research project (Sherizadeh, 2023), it was necessary to establish an appropriate approach for simulating the stress changes associated with abutment loading. For this purpose, the approach developed by Barczak et al. (2008) was followed to simulate the side and face abutment loading stages beyond the initial development phase for each model scenario.

For each parametric scenario, the model was first solved under development conditions and converged. After the development stage converged, the strength reduction method was applied to determine the development RibFOS. The vertical stress was then increased by 20%, and the horizontal stress was reduced by 20% to simulate side abutment loading conditions. The model was solved to equilibrium, and the strength reduction method was applied to determine the side-abutment RibFOS. The final modeling stage represented face abutment loading. Relative to the model's development-stage stress conditions, the face abutment loading conditions were simulated by increasing the vertical stress by 120% and the horizontal stress by 20%. The model was again solved to equilibrium, and the strength reduction method was used to determine the face-abutment RibFOS for each scenario. This approach was consistent with that employed by Barczak et al. (2008).

Figure 23 illustrates the development, side, and face abutment loading responses for an illustrative parametric model case with an overburden depth of 800 ft, mining height of 11 ft, and development RibFOS of 0.77. Under development conditions, an ultimate mid-rib displacement of 5.5 mm can be seen at point 1. After increasing the vertical stress applied to the model by 20%, point 2 illustrates the response under side abutment conditions. While there is an observable increase in rib displacement, this increase is minimal, with the ultimate rib displacement increasing from 5.5 to 6 mm. Similarly, there is a slight increase in the mobilized zone depth between the development and face abutment conditions owing to the increase in applied vertical stress. In contrast to the relatively small increase between points 1 and 2, point 3 in Figure 23 illustrates a substantial increase in predicted rib deformation resulting from face abutment loading conditions. Comparing the rib deformation predicted under side and face abutment conditions, the displacement nearly doubles from 6 mm to approximately 11.75 mm. Similarly, the rib deformation zone becomes considerably larger, indicating significant instability compared to the previous stages. This behavior is consistent with both the progression of vertical load increase as an excavation

transitions from development to side abutment and face abutment conditions and observations noted by Zhang et al. (2017).

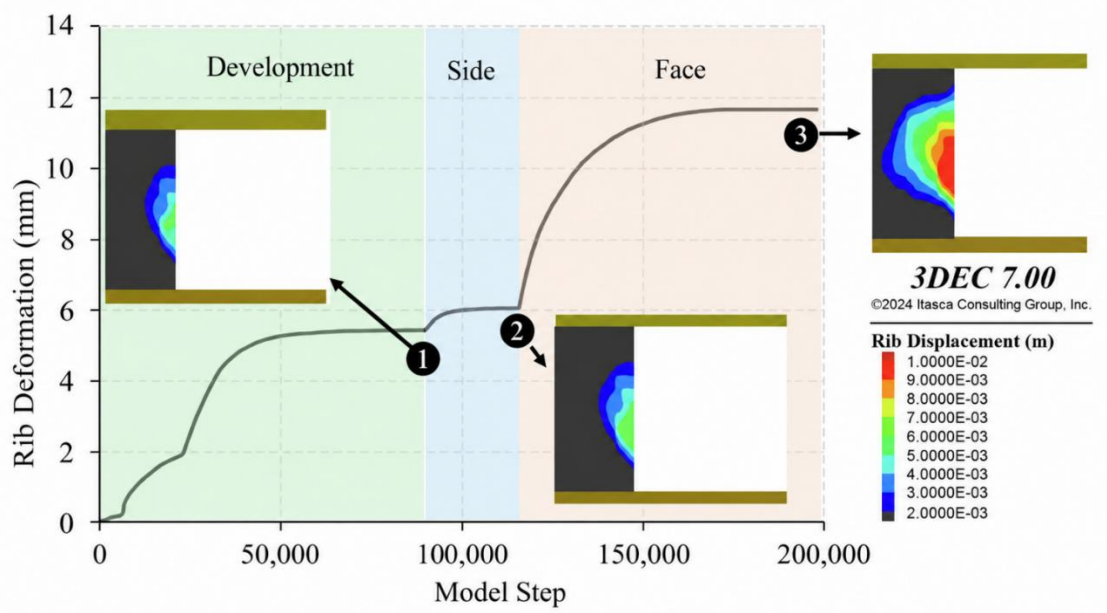


Figure 23: Three stages captured in the abutment loading parametric study: (1) Development Conditions, (2) Side Abutment Conditions, and (3) Face Abutment Conditions.

To develop a relationship between RibFOS and abutment loading conditions, the parametric model results were plotted, and regression relationships were fitted to the side- and face-abutment datasets. Figure 24 illustrates that the regression models effectively capture the relationships between development RibFOS and RibFOS under the two abutment loading conditions. For side abutment loading conditions, the development RibFOS is reduced by 19%, whereas face abutment loading reduces the development RibFOS by 64%. Comparing these two reductions demonstrates the substantially greater effect of face abutment loading on RibFOS relative to side abutment loading.

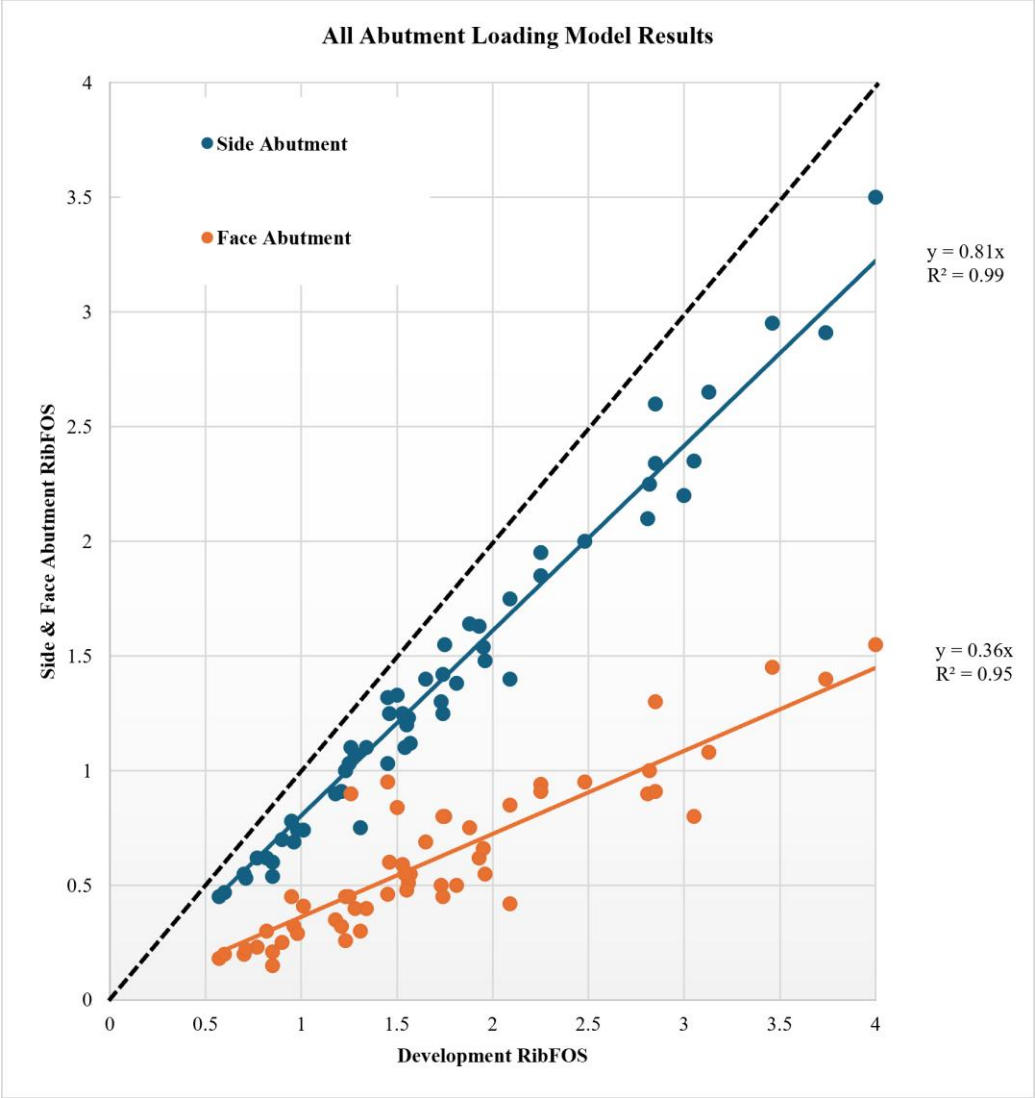


Figure 24: RibFOS results for side and face abutment loading conditions for various coal rib configurations.

Exploration of Rib-Corner Stability and Support Configurations

Based on the 58 base 2D parametric model scenarios, 10 scenarios were selected for 3D corner modeling. The criterion for selecting the 10 cases was based on the predicted unsupported RibFOS from the development stage of the 2D parametric model scenarios. The 10 selected cases targeted scenarios in which the unsupported RibFOS fell between 1.0 and 2.0. This was done to exclude cases with RibFOS below 1.0, where mid-rib instability could overshadow the response of the corner. Similarly, models with unsupported RibFOS values greater than 2.0 were excluded, as minimal damage was observed at the pillar corner. The resulting subset of 10 scenarios for the 3D corner stability models is shown in Table 3.

Table 3: Selected scenarios for 3D corner models.

Scenario	*Coal Type*	*Depth (ft)*	*Mining Height (ft)*	*Parting Type*	*Parting Thickness (ft)*	*CPRR*	*Development RibFOS*
1	*DC-DC*	*1050*	*11*	*Weak*	*3.85*	*79*	*1.21*
2	*DC*	*1050*	*11*	*---*	*---*	*94*	*1.23*
3	*BBC*	*600*	*11*	*---*	*---*	*50*	*1.46*
4	*DC-DC*	*1050*	*9*	*Weak*	*3.15*	*79*	*1.56*
5	*BBC-BBC*	*600*	*9*	*Weak*	*1.8*	*60*	*1.65*
6	*BBC*	*800*	*7*	*---*	*---*	*50*	*1.73*
7	*BBC-DC*	*1050*	*7*	*Weak*	*2.45*	*75*	*1.74*
8	*BBC*	*600*	*9*	*---*	*---*	*50*	*1.75*
9	*DC*	*800*	*11*	*---*	*---*	*94*	*1.88*
10	*BBC-DC*	*900*	*9*	*Weak*	*3.15*	*70*	*1.96*

The 3D corner modeling efforts were conducted in two phases. In the first phase, the 10 corner scenarios were evaluated without support to characterize rib-corner response under the selected mining and geological conditions. In the second phase, support configurations were explored, first using Scenario 6 to evaluate alternative bolting patterns and then applying the selected pattern to the remaining scenarios. For the unsupported corner models, the deformation-based stability criterion was used to identify the formation and extent of the mobilized zone as a metric for evaluating corner stability. This was achieved by generating an isosurface for each corner model that captured elements with a displacement greater than 1 cm (0.4 in). The isosurfaces were then trimmed to retain regions where the depth of mobilization exceeded 25 cm (9.8 in), consistent with the deformation-based stability criterion. The processed isosurfaces were used to determine the mobilized-zone volume.

Because the modeled scenarios included both single-solid coal ribs and ribs containing rock partings, mobilized volume was used as the common metric for comparison among all scenarios. Applying a single density to the entire mobilized zone would not account for the different densities of coal and rock where both materials were present. For single-solid coal scenarios, mobilized-zone mass was estimated using an assumed coal density of 1,300 kg/m³ (81.2 lb/ft³). A density of 2,500 kg/m³ (156.1 lb/ft³) was assumed for shale or rock partings. The unsupported models provided insight into the pillar-corner response under the selected mining and geological conditions. One key insight obtained from the unsupported corner models was that increasing rib height, with all other parameters held constant, notably increases corner instability. Figure 25 illustrates this by comparing two representative cases in which all parameter levels are held constant except rib height.

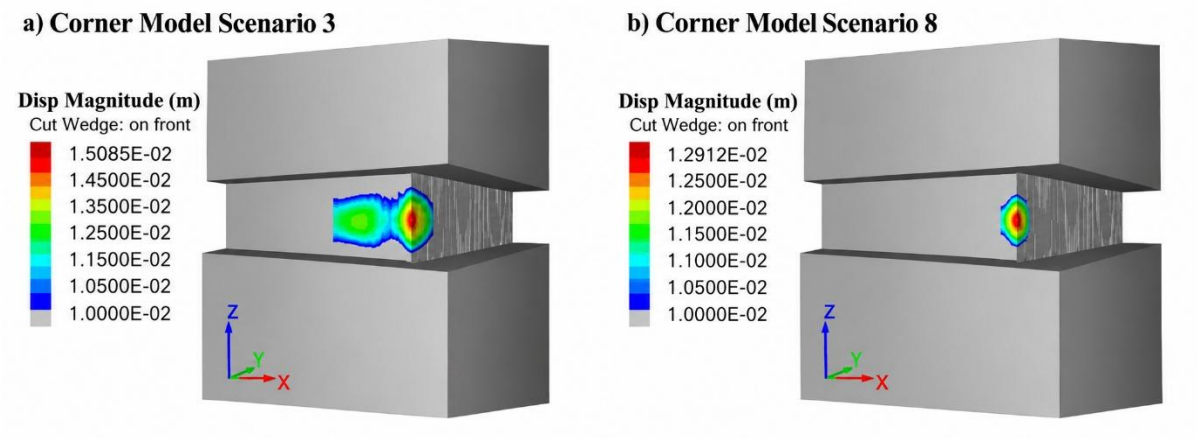


Figure 25: Displacement magnitude responses for a) single-solid BBC, 600 ft overburden depth, and 11 ft rib height and b) single-solid BBC, 600 ft overburden depth, and 9 ft rib height.

Figure 25a.) shows a much larger mobilized zone formation at the pillar corner than Figure 25b.) which shows a significantly smaller mobilized zone at the corner edge. Scenario 3 had a mobilized-zone volume of approximately 2.20 m³, whereas Scenario 8 had a mobilized-zone volume of approximately 0.231 m³. Because both scenarios consist of single-solid BBC, using the assumed coal density of 1,300 kg/m³ gives estimated mobilized masses of approximately 2,857 kg (6,298 lb) and 300 kg (661 lb), respectively. The difference in mobilized volume and estimated mass between these two scenarios is approximately 9.5-fold, illustrating the significant impact of rib height on corner stability. At larger rib heights, more material is excavated, removing more confinement from the coal pillar surfaces and exposing the corner to greater levels of induced stress relief from both the crosscut and entry rib surfaces.

The mobilized-zone volumes for the unsupported simulations of the 10 corner scenarios are presented in Table 4. These mobilized-zone volume values were used as a baseline to evaluate corner support patterns and their effectiveness in improving rib corner stability.

Table 4: Unsupported corner model estimated mobilized-zone volume.

Scenario	Mobilized Zone Volume (m³)
1	9.203
2	9.652
3	2.198
4	3.342
5	0.386
6	0.866
7	1.923
8	0.231
9	3.863
10	1.961

After establishing the unsupported mobilized-zone baselines for the corner model scenarios, multiple bolting patterns were explored to identify which was most effective. Support element properties from our previous Alpha Foundation project were used to simulate the fully grouted

bolt behavior (Sherizadeh et al., 2024). To model the support installation, the same model solution steps outlined above were followed until the boundary force relaxation stage of the excavation. The boundary forces were softened by 10% using the nonlinear function, and then the bolt elements were installed in the rib for the current excavation stage. The boundary forces were then fully relaxed as previously described. Finally, the model excavation stage was solved to equilibrium. This process was repeated for the second excavation stage to simulate the bolting cycle steps observed in the field. The boundary forces were softened by 10% before installing the support elements to ensure that the support elements were fully engaged in the corner models. Initial exploration illustrated that the mining conditions in the modeling scenarios would not exceed the load capacity of the fully grouted bolts. Corner model Scenario 6 was used to explore potential corner support designs before testing on the remaining 9 scenarios.

The first corner support pattern involved using one 5-ft-long, fully grouted bolt, installed in the mid-rib, per vertical column with a horizontal spacing of 8 ft between columns. The first bolt column was installed 1.5 m (5 ft) from the corner edge to place the bolts as close to the corner edge as possible while ensuring the support elements did not collide in the model. Figure 26 illustrates the mobilized-zone isosurface together with the bolt response for scenario 6 under unsupported and supported conditions for the first corner support design.

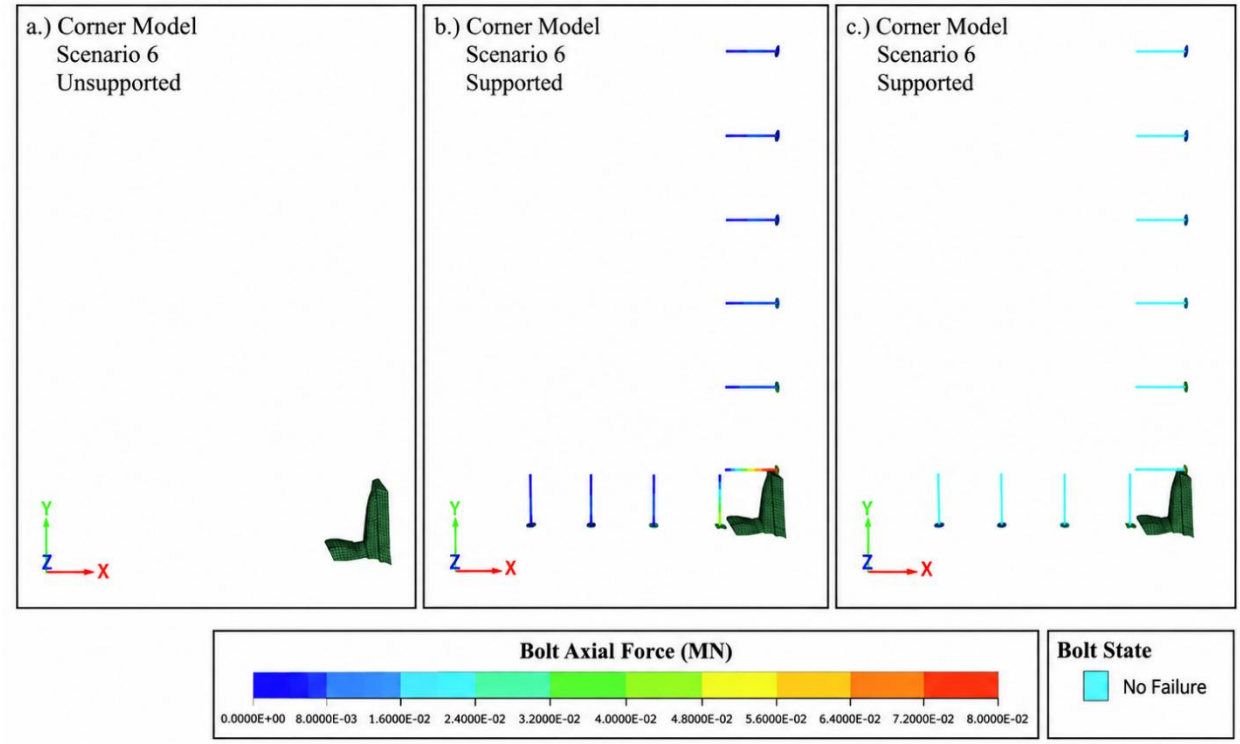


Figure 26: a.) Unsupported, b.) Supported design case 1 bolt axial force, and c.) Supported design case 1 bolt states.

Comparing the isosurfaces for the unsupported and supported models, this bolting design showed minimal effect. The two bolts closest to the corner edge on the crosscut and entry ribs show signs

of engagement, but the other bolts show minimal signs of activation. Furthermore, the size of the mobilized zone is not notably reduced when support is installed. The mobilized-zone volume decreased from 0.866 m³ in the unsupported case to approximately 0.719 m³ in the supported case. Because Scenario 6 is a single-solid BBC rib, these volumes correspond to estimated coal masses of approximately 1,125 kg (2,481 lb) and 935 kg (2,061 lb), respectively, using the assumed coal density of 1,300 kg/m³. These results indicated that individual bolt support was not effective at stabilizing the corner region. This was particularly true for this first corner support design, as the bolts were not passing through the mobilized zone and therefore could not resist mobilization in the rib.

The next bolt pattern tested on corner model Scenario 6 aimed to increase support density at the corner and explore whether this increase improved corner stability. This was achieved by taking the first support design and increasing the number of bolts per column from 1 to 3 while within 10 ft of the corner edge. This resulted in three 5-ft-long fully grouted bolts – uniformly spaced vertically in the rib – per vertical column with a horizontal spacing of 8 ft between bolt columns. The first bolt column in the entry and crosscut was installed 5 ft from the pillar corner edge to prevent collisions between the support elements in the model, as in the first design. Figure 27 illustrates the mobilized-zone isosurface and bolt response for this support configuration relative to the unsupported case.

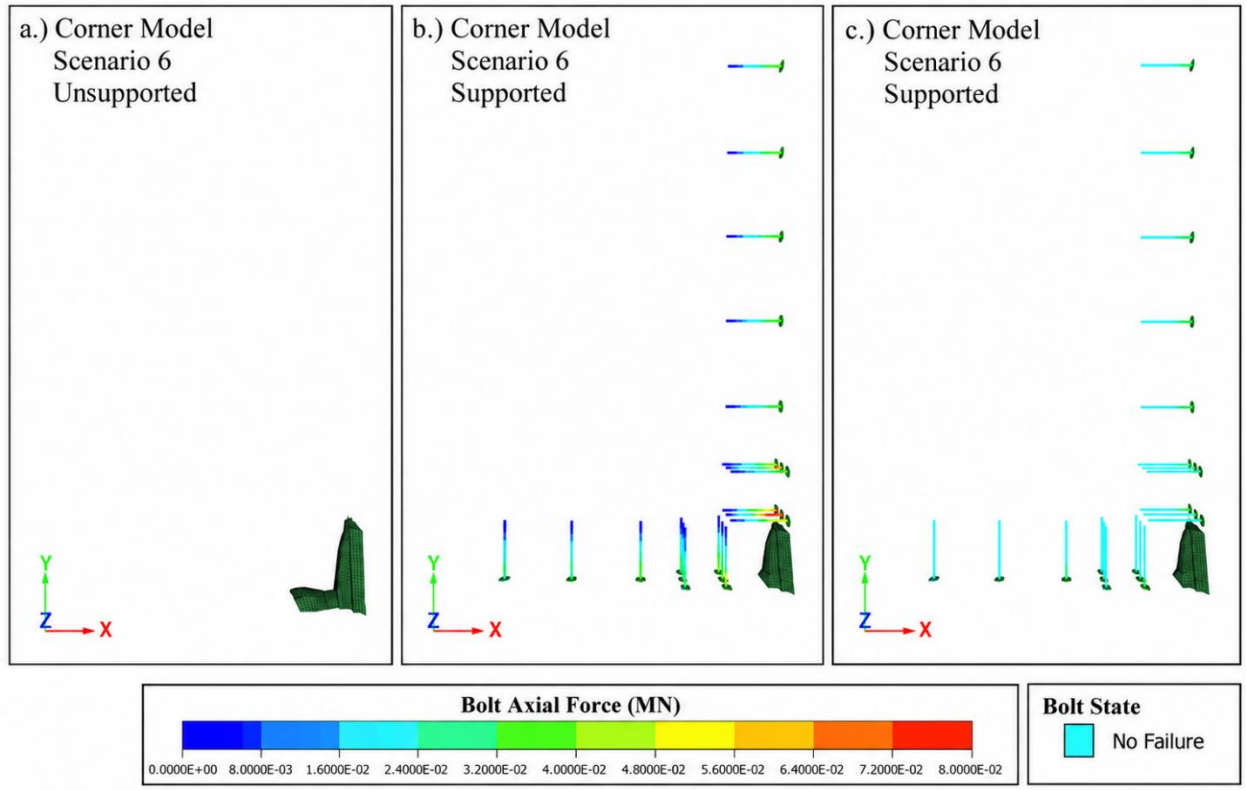


Figure 27: a.) Unsupported, b.) Supported design case 2 bolt axial force, and c.) Supported design case 2 bolt states.

Unlike the first support design case, increasing the density of the bolts near the corner edge showed a noticeable reduction in the size of the mobilized zone at the corner. After increasing the support density near the corner edge, the mobilized-zone volume decreased from 0.866 m^3 to approximately 0.482 m^3. For this single-solid BBC scenario, the corresponding estimated mobilized mass decreased from approximately 1,125 kg (2,481 lb) to 626 kg (1,380 lb). While there is a notable reduction in corner instability for this model scenario, there is still a sizable mobilized zone on the entry-side and immediate corner edge, extending 1.32 m (4.33 ft) from the corner edge along the entry. This persistent instability indicates that bolt location is another key parameter beyond support density when supporting the corner.

The third support design case combined the findings from the first two attempts by increasing support density and positioning bolts to maximize proximity to the corner edge. The outcome was an asymmetric bolt pattern: 2 bolts per column in the entry and 1 bolt per column in the crosscut while within 10 ft of the corner edge. Furthermore, the horizontal bolt spacing was reduced from 8 ft to 2 ft to provide higher support density. It is important to note that the orientation of the asymmetric bolting pattern is a critical consideration. In the corner models, the maximum horizontal stress is oriented parallel to the entry. This stress orientation results in less favorable rib conditions in the entry rib compared to the crosscut rib. Because the entry-side of the pillar experiences less favorable conditions in the numerical models, two 5-ft-long bolts were installed per vertical column with uniform vertical spacing. One 5-ft-long bolt was installed in the crosscut at the mid-rib of the pillar. If the horizontal stress orientation were reversed, 2 bolts per column would need to be installed in the crosscut corner rib, and 1 bolt per column would need to be installed in the entry rib. Given the vertical spacing of the bolts in the entry rib, it is possible to install the crosscut bolts between the entry bolts and prevent collisions of the bolt elements. This allowed the first column of bolts in the entry and crosscut to be placed much closer to the corner edge than previous support designs. The bolt pattern design tested in the third case was: two 5-ft-long fully grouted bolts installed with uniform vertical spacing per column, with the first column installed 2 ft from the corner edge and a horizontal spacing of 2 ft along the entry rib. The crosscut used the same horizontal spacing and distance from the corner, but with one bolt per column placed at the mid-rib. Figure 28 provides a comparison of the unsupported and supported isosurfaces with a plot of the bolt axial force and state.

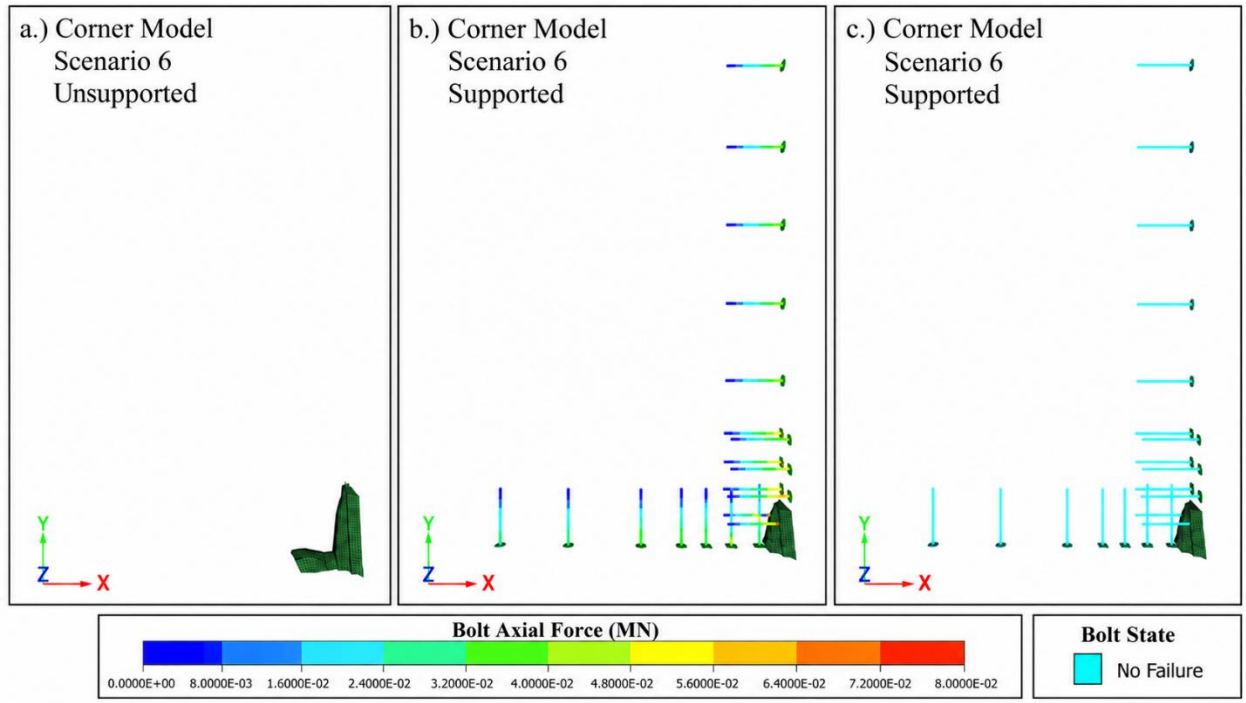


Figure 28: a.) Unsupported, b.) Supported design case 3 bolt axial force, and c.) Supported design case 3 bolt states.

Comparing the size of the mobilized zone using this bolting design, there is a significant reduction in corner instability when the support pattern is installed. The mobilized-zone volume decreased from 0.866 m^3 in the unsupported case to approximately 0.292 m^3 in the supported case. Using the assumed coal density of 1,300 kg/m^3, the corresponding estimated mobilized mass decreased from approximately 1,125 kg (2,481 lb) to 380 kg (837 lb). With this support pattern design, the unstable region of the corner is reduced in size, extending 0.9 m (2.95 ft) from the corner edge along the entry, and installing rib mesh on the surface of the corner could potentially stabilize the corner. The results of this case compared to the previous two indicate that support density plays the greatest role in stabilizing the corner, and support positioning enhances the support density effect when comparing case 3 to the previous two cases. After identifying case 3 as the most successful pillar corner support design, this pattern was applied to the remaining 9 scenarios to evaluate the pattern's generalizability across the selected corner modeling cases. Table 5 compares the unsupported and supported corner mobilized-zone volumes for all 10 corner model scenarios.

Table 5: Unsupported and Supported rib corner mobilized-zone volume.

Scenario	Unsupported Volume (m^3)	Supported Volume (m^3)
1	9.203	9.202
2	9.652	7.506
3	2.198	0.962
4	3.342	2.296
5	0.386	0.165
6	0.866	0.292
7	1.923	1.295
8	0.231	0.075
9	3.863	3.553
10	1.961	1.052

Comparing the unsupported and supported mobilized-zone volumes for each scenario, a few scenarios show little change after support installation. Specifically, Scenario 9 illustrates an inherent limitation of the modeling methodology used to capture the pillar corner behavior. Figure 29 illustrates plots of the element states, accumulated shear plastic strain, and accumulated tensile plastic strain for this case.

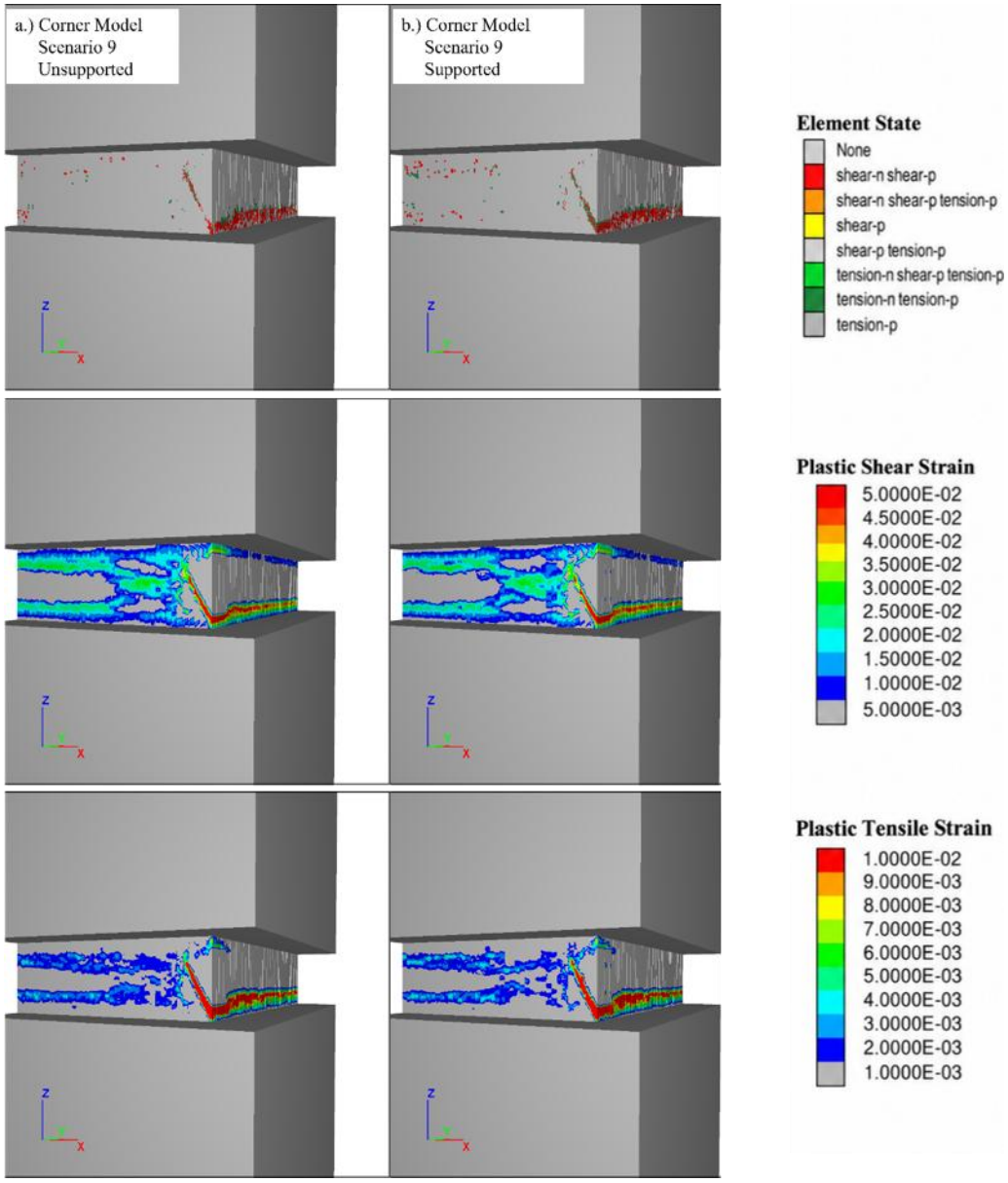


Figure 29: Plots of element states, accumulated plastic shear strain, and accumulated plastic tensile strain for corner model Scenario 9.

Comparing the unsupported and supported model plots for Scenario 9, there is little difference in the plastic response of the two models. This indicates that the installed support elements are not providing a substantial support effect in the supported model. Referring to Table 3, Scenario 9 consists of a single-solid DC lithotype rib configuration. The plots in Figure 29 indicate that a failure plane has formed in the coal matrix rather than explicit separation of the face and butt cleat joints due to the relatively higher strengths of the cleat systems in the models. Given the hybrid nature of the 3DEC solver, it is possible for support elements to contribute little to the model response if the solution is primarily continuum mechanics based (Sinha & Walton, 2019). The limited efficacy of the support elements in the corner model scenarios with the DC lithotype is largely attributed to this methodological limitation.

Comparing the unsupported and supported mobilized-zone volumes for the remaining scenarios in Table 5 generally shows improved corner stability with the asymmetric bolt pattern described in support design case 3 (Figure 28). These results indicate that the asymmetric configuration is a potentially effective corner-support pattern within the conditions represented by the selected models. The modeling also indicates that rib mesh may provide useful supplemental surface support within approximately 10 ft of the corner where a residual mobilized region remains after bolting.

These findings should be considered preliminary rather than prescriptive. The corner models were restricted by the lack of field data for explicit calibration, and the results do not comprehensively evaluate corner stability. Further work is needed to establish a quantitative corner-stability criterion and to validate the modeled support response against field measurements. Similarly, given the small sample set for the corner modeling scenarios and the complexity of the modeling methodology, the corner support recommendation is initial and does not establish a fully developed corner support design criterion. Based on the 10 corner modeling scenarios, the selected corner support design showed potential for improving corner stability and provides a basis for further field evaluation and model validation.

3.3. Objective 3: Integrate MSI, Abutment Loading, and Rib-Corner Stability into the Coal Rib Control System

3.3.1. Task #5. Integration of Project Outcomes into the Rib Support Recommendation Tool (RSRT)

The outcomes of our previous Alpha Foundation research project included developing a stand-alone application, the RSRT application, that directly incorporates the developed charts, tables, and relationships based on the parametric modeling analysis and expansion of the CPRR system's capabilities (Sherizadeh et al., 2024). As part of the integration phase of this research project, the RSRT application was transferred from its original MATLAB-based application platform to a Python-based platform to improve the usability of the software, interfaces, application workflow, and facilitate effective incorporation of this research project's outcomes. The new RSRT version retained the original capabilities of the previous versions and added the ability to handle MSI effects, abutment loading conditions, and corner support recommendations based on the outcomes of this research. The main interface of the updated RSRT application is shown in Figure 30, where an improved dashboard provides the user with more information than was originally available. The aim of developing this application was to facilitate coal mine operators' use of the coal rib control system's tables and charts developed in our previous research efforts. Direct usage of the tables and charts is possible, but due to the scale of parameters necessary to determine CPRR values, development RibFOS estimates, and rib support recommendations, it is more efficient and user-friendly to facilitate these tasks through this application.

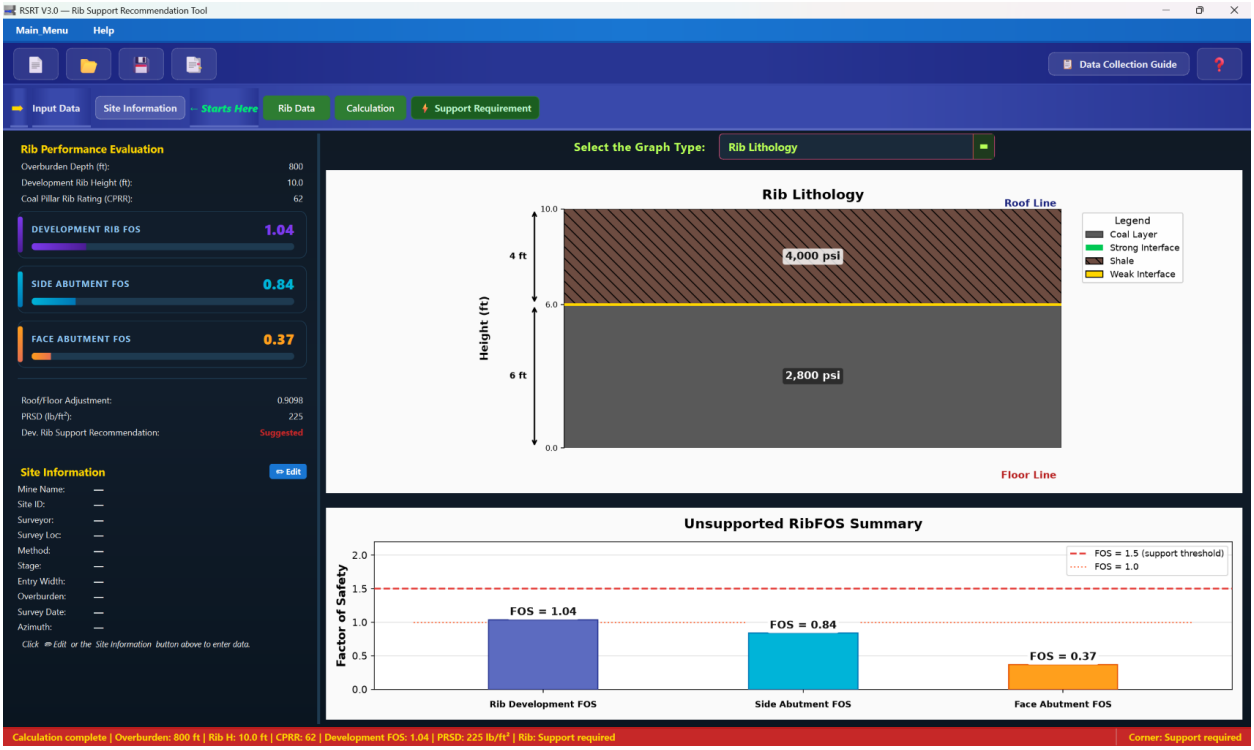


Figure 30: The updated RSRT application main interface presenting development, side, and face abutment RibFOS results, alongside a rib lithology chart based on user inputs.

The relationships built into the RSRT application to evaluate site-specific coal rib properties, including CPRR values and development RibFOS estimates, have not been adjusted or changed from the previous research project. These relationships were directly incorporated into the updated version of the RSRT application. The new capabilities of this application focus on adjusting RibFOS estimates based on MSI effects and abutment loading conditions and providing preliminary coal rib corner support recommendations based on the outcomes of this research. To integrate MSI effects into the application, Equation 8 was directly incorporated to link percent vertical stress increases caused by MSI, as determined through the ACPS software, to a RibFOS adjustment, as detailed above. When the user is evaluating MSI effects, they simply input the percent vertical stress increase, and the application computes the RibFOS adjustment and applies it to the development RibFOS. The adjusted RibFOS is then used to determine rib support requirements and recommendations for the specific site conditions provided by the user. Similarly, for abutment loading conditions, the user can select between side or face abutment loading conditions, where a RibFOS multiplier of 0.81 or 0.36 is used, respectively, to reduce the development RibFOS, as outlined above. The adjusted RibFOS is then used to determine rib support requirements and recommendations for the specific site conditions provided by the user.

Figure 31 and Figure 32 illustrate the updated RSRT site-specific rib support recommendations interfaces for evaluating MSI effects and abutment loading conditions, respectively. For all evaluation modes, a plot of the primary rib support density (PRSD) against the unsupported RibFOS is shown to allow for quick visual comparison against a database of U.S. coal mine case

histories for rib support. Based on data collected by Mohamed et al. (2021b), curves representing maximum, average, and minimum relationships between PRSD and unsupported RibFOS were created to facilitate rib support recommendations. Our previous Alpha Foundation project identified that PRSD is not sufficient as a design parameter for rib support, as different rib support patterns can provide the same PRSD value while ineffectively interacting with the coal rib (Sherizadeh et al., 2024). To remedy this, the PRSD value is used to link the calculated unsupported RibFOS to the relationships and support tables generated in our previous Alpha Foundation project and provide a means of generating site-specific support recommendations. Equation 9, developed in the work completed by Mohamed et al. (2021b), provides the empirical relationship between PRSD and specific bolt parameters.

$$PRSD = \frac{\tau_{rb} \times N}{S \times H} \tag{9}$$

where τ_{rb} is the anchorage capacity of the rib bolt in short lb., N is the number of bolt rows, S is the horizontal spacing between bolts in feet, and H is the mining height in feet. The recommended bolt length is determined from Equation 10, and the number of bolt rows is determined from Table 6.

$$Bolt\ Length\ (L, ft) = 0.5\ \times H + 1 \tag{10}$$

Table 6: The number of bolt rows based on the rib height and estimated RibFOS

Rib Height (H, ft)	RibFOS	Number of Bolt Rows (N)
H ≤ 7	RibFOS ≤ 1.5	1
7 < H ≤ 9	RibFOS ≤ 1.0	2
	1.0 < RibFOS ≤ 1.5	1
9 < H < 10	RibFOS ≤ 1.5	2
10 ≤ H	RibFOS ≤ 1.0	3
	1.0 < RibFOS ≤ 1.5	2

To determine horizontal bolt spacing, Equation 9 was rearranged and used to solve for S, as seen in Equation 11. PRSD estimates from the average curve relating PRSD and RibFOS, bolt length from Equation 9, and the number of bolt rows from Table 6 are used to solve for S. The anchorage capacity is held constant, assuming Grade 60 and 5/8 inch rib bolts.

$$S = \frac{\tau_{rb} \times N}{PRSD \times H} \tag{11}$$

The RSRT application directly employs Equations 10 and 11 and Table 6 to provide a site-specific rib support recommendation based on estimated RibFOS and case-history-defined PRSD requirements.

Specifically, when evaluating abutment loading conditions, a plot of abutment RibFOS against development RibFOS appears with both side and face abutment trendlines to facilitate quick visual comparison of the side- and face-abutment RibFOS relationships.



Figure 31: Site-specific support recommendations evaluating a vertical stress increase of 30% from MSI effects.



Figure 32: Site-specific support recommendations evaluating side abutment loading conditions.

The recommended support pattern is dependent on the site conditions, required PRSD based on the case-history trendline, and RibFOS value. The tables relating mining and geological conditions to RibFOS values developed as an outcome of our previous Alpha Foundation research project are directly referenced and used to provide the applicable support recommendation to improve the RibFOS above a value of 1.5 if necessary. These recommendations are still based on the extensive parametric modeling and analysis linking unsupported RibFOS values with site-specific conditions developed in our previous research efforts.

The final updated component of the RSRT application is the rib corner support recommendation tab. Based on the 3D modeling efforts conducted as part of this research project, the selected support configurations showed potential for improving rib-corner stability within the modeled cases. Because the corner models were not directly calibrated against field measurements and were limited to the selected scenarios, the resulting corner support guidance is considered preliminary. The updated RSRT application accounts for this and provides a separate corner support interface to provide preliminary guidance for configuring the corner support pattern, based on the outcomes of the selected 3D corner modeling efforts detailed above. Figure 33 illustrates the corner support interface.

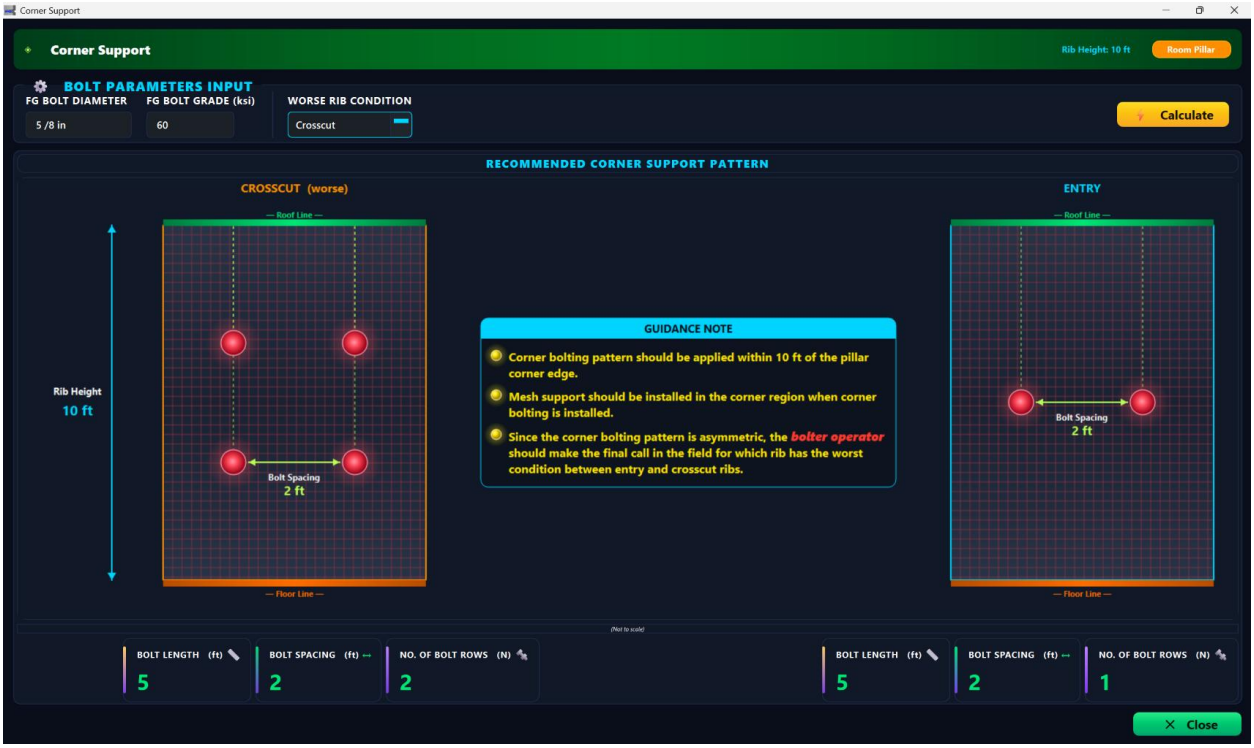


Figure 33: Corner support interface for preliminary coal rib corner support patterns.

The corner support interface provides two displays for the crosscut and entry faces of the corner. Since the preliminary recommended bolt pattern is asymmetric, it is necessary to account for the rib conditions before installing the corner support. The guidance note states that final support decisions should be made on site, and the interface also provides a user-selected dropdown box to identify which of the entry and crosscut ribs has the worse condition. Considering it is not feasible to directly measure in-situ horizontal stresses across all pillars at an active mine during support installation cycles, this field-based selection provides a practical proxy for identifying which rib should receive the higher-density portion of the asymmetric corner support pattern.

The outputs of the RSRT application are site-specific rib support recommendations building on the work completed in our previous Alpha Foundation project (Sherizadeh et al., 2024). The work of this project included accounting for the effects of MSI and abutment loading conditions on unsupported RibFOS, allowing for rib support recommendations that reflect these conditions.

3.3.2. Task #6. Field-Case Evaluation of the Updated Rib Support Recommendation Tool (RSRT)

In this section, the support practices implemented at two of the active mine sites surveyed are compared with the support systems recommended by the RSRT tool to evaluate the updated RSRT after incorporating MSI and abutment loading effects. The two active cases were selected from the site survey locations detailed in Section 3.1.1 of this report, with a focus on capturing MSI effects and abutment loading conditions observed in the field. The goal of the field-case evaluation was

to compare the updated RSRT outputs with documented field conditions and the rib support practices used at the surveyed sites.

The first case, a mine operating in the Eagle Seam, was selected due to significant MSI effects being observed at the site survey location. This provides a basis for comparing RSRT outputs that account for MSI with the support design and rib conditions documented at the mine. The second case was selected because significant abutment loading conditions were observed during the site surveys. Case 2 was therefore used to evaluate the RSRT response when side abutment loading is incorporated into the rib stability assessment.

The site details used for both field cases are provided in Table 7 and Table 10, rather than using the broader seam-wide conditions described in the field survey section. It is important to note that the No. 2 Gas case uses an overburden depth of 1,100 ft, which lies outside of the model bounds used to define the RSRT application. Similarly, the shale-unit UCS values reported in the Eagle case fall below the values used to develop the numerical modeling database. Accordingly, these cases should not be interpreted as validating application of the RSRT outside the established parameter ranges of the underlying relationships. The comparisons are intended specifically to evaluate the incorporation of MSI and abutment loading effects into the updated RSRT.

Case 1: Eagle Seam

For the first field case, the mine active in Eagle Seam was selected due to severe MSI effects associated with the approximately 30 ft interburden between the active Eagle workings and the previously mined Upper Eagle Seam. The overburden depth at the survey location is 1,050 ft. The rib was measured as 8.25 ft tall and consists of three units, with a coal layer sandwiched between an upper and a lower shale unit. A weak interface was identified at both contacts between the coal and the shale. Details of the rib composition, including the unit thicknesses and material strengths, are summarized in Table 7. Considering the severe conditions observed at the survey location, the rib was supported using two rows of fully grouted Grade 60 bolts, 5 ft long, with a measured spacing of 4 ft between bolts.

Table 7: Rib details and mining conditions for the surveyed pillar in Case 1.

Parameter	Value
Overburden depth (ft)	1,050
Rib height (ft)	8.25
Rib unit 1	Shale, 3.0 ft, 2,000 psi
Rib unit 2	Coal, 2.83 ft, 1,500 psi
Rib unit 3	Shale, 2.42 ft, 2,000 psi
Weak or strong interfaces	Weak at both contacts with the coal

The rib composition data given in Table 7 were entered into the RSRT tool, which returned a Coal Pillar Rib Rating of 29 and an unsupported development RibFOS of 0.20. Using the ACPS software to evaluate the percent vertical stress increase caused by MSI, a value of 62.1% was used to define the MSI adjustment in the RSRT application. After adjusting the development RibFOS based on the estimated MSI effects, the unsupported development RibFOS fell further to 0.08, and the recommended PRSD rose from 654 to 758 lb/ft² (Table 8). Based on these values, the tool recommends two fully grouted bolts, 5 ft long, spaced 4 ft apart, and it also recommends secondary support such as welded wire mesh for this case.

Table 8: RSRT output summary for Case 1, Eagle Seam.

Parameter	Value
Estimated Coal Pillar Rib Rating	29
Development RibFOS, unsupported	0.20 (0.08 when accounting for MSI)
Primary Rib Support Density, development (lb/ft^2)	654 (758 when accounting for MSI)

Figure 34 shows the RSRT calculation output for this case, and Figure 35 shows the corresponding support recommendation once the multiple seam interaction adjustment is applied. As the figures show, the recommended primary support system matches the active primary support practice at the selected field location in the number of bolts, bolt length, and spacing. Beyond the mine's primary support practice, the RSRT application recommends secondary support for the severe rib conditions represented by this case, rather than changing the primary bolting pattern. Table 9 shows the comparison of applied support in the field and RSRT tool recommendations.

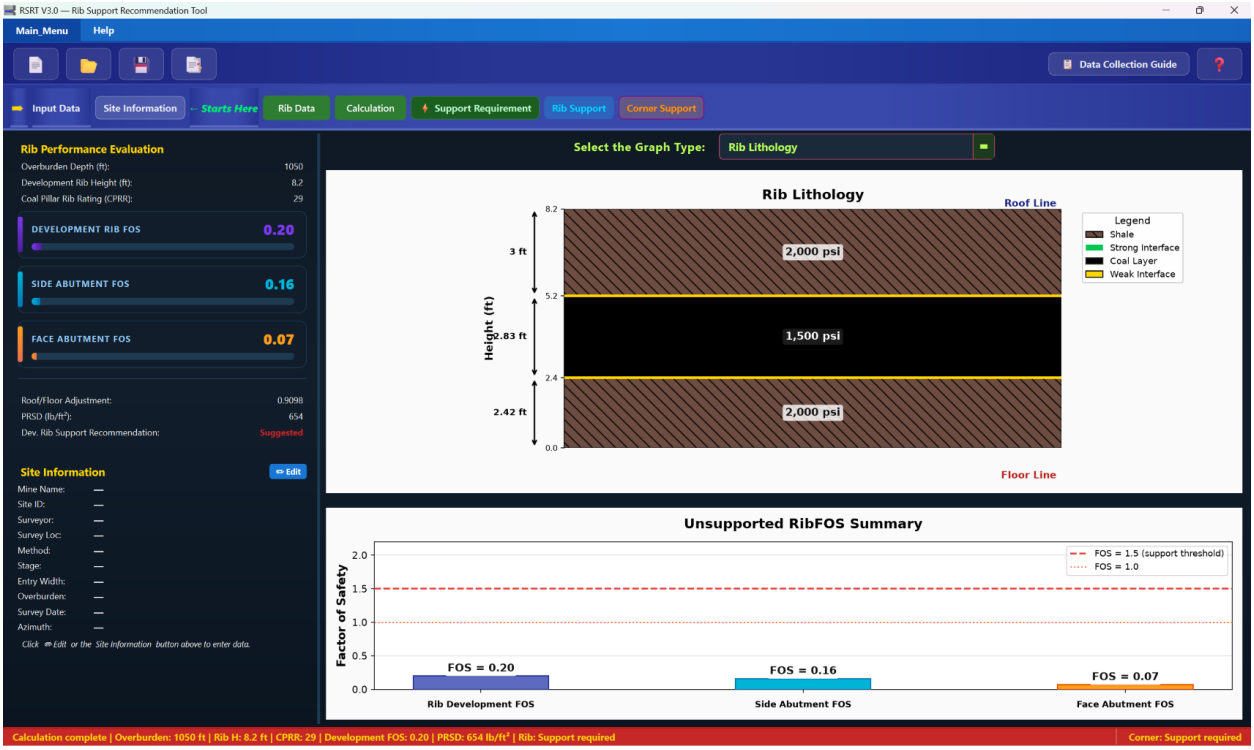


Figure 34: RSRT calculation output for the Eagle seam case, showing an overburden depth of 1050 ft, a Coal Pillar Rib Rating of 29, and unsupported development RibFOS value of 0.20.



Figure 35: RSRT support recommendation for the Eagle seam case under development loading, with the multiple seam interaction adjustment applied.

Table 9: Case 1, Eagle Seam comparison of active mine support at the selected field location and the RSRT recommendation.

Parameter	Active support (mine)	RSRT recommendation, development
Number of bolts	2	2
Bolt length (ft)	5	5
Spacing (ft)	4	4
Bolt type	Fully grouted	Fully grouted
Secondary support	Not used	Required

The primary support recommendations from the RSRT application directly match the primary support pattern used by the mine at the selected field location. One notable output from this field case is that the RSRT recommends using secondary support, such as welded wire mesh, in addition to the primary support pattern detailed in Table 9. The broader Eagle Seam survey documented the use of additional timber support at some locations where formed brows occurred. Table 9, however, represents the support configuration documented at the specific location selected for this RSRT evaluation.

Case 2: No. 2 Gas Seam

In the second case, the coal being mined is part of the No. 2 Gas Seam, at an overburden depth of 1,100 ft. No significant MSI is expected at this location based on site observations, and this assumption was used when inputting site details into the RSRT application. The rib is 7 ft tall and consists of three units: an upper shale unit, a coal unit, and a thin lower shale unit, with a weak interface above the coal and a strong interface below it. Details of the rib composition are given in Table 10. In this mine, the active support plan installs a single row of fully grouted Grade 60 angled bolts, 5 ft long, at roughly 8 ft spacing, installed into the top shale unit whenever its thickness is greater than 2 ft. No bolts were installed in the coal unit, and rib brows have been observed at several pillar corners in this seam.

Table 10: Rib details and mining conditions for the surveyed pillar in Case 2.

Parameter	Value
Overburden depth (ft)	1100
Rib height (ft)	7.0
Rib unit 1	Shale, 2.5 ft, 4000 psi
Rib unit 2	Coal, 4.0 ft, 2250 psi
Rib unit 3	Shale, 0.5 ft, 4000 psi

Parameter	Value
Weak or strong interfaces	Weak above the coal, strong below it

The rib composition data were entered into the RSRT tool, which returned a CPRR of 48 (Figure 36 and Table 11). Because this rib was evaluated under development and side abutment conditions, the RSRT application returned an unsupported RibFOS of 0.56 and 0.45 for these two loading stages. Rib support is necessary because the unsupported RibFOS in development and side abutment conditions falls below the 1.5 RibFOS support threshold. Under development loading, the tool recommends a single fully grouted bolt, 4 to 5 ft long, spaced 4 to 6 ft apart (Figure 37).

The RSRT support recommendation is intended to improve overall rib stability and reduce the potential for brow formation by limiting coal-rib sloughage. The recommended development-conditions rib support pattern, based on the established rib support design criteria in our previous research (Sherizadeh et al., 2024), places fully grouted support at the mid-rib with tighter spacing, rather than limiting the support to the upper shale unit as practiced at the mine under development conditions.

Once the rib comes under side abutment loading, however, the recommended support changes notably. For the more complex abutment loading stage, the tool calls for two fully grouted bolts, 5 ft long, spaced 4 ft apart (Figure 38). This recommendation reflects the reduction in RibFOS from 0.56 under development conditions to 0.45 after accounting for side abutment loading. The expanded RSRT application accounts for this by reducing the development RibFOS based on the abutment conditions, and it provides a denser support pattern corresponding to the lower adjusted RibFOS. The resulting support recommendation is intended to improve rib stability under the increased loading condition and reduce the potential for coal sloughage and associated brow formation.

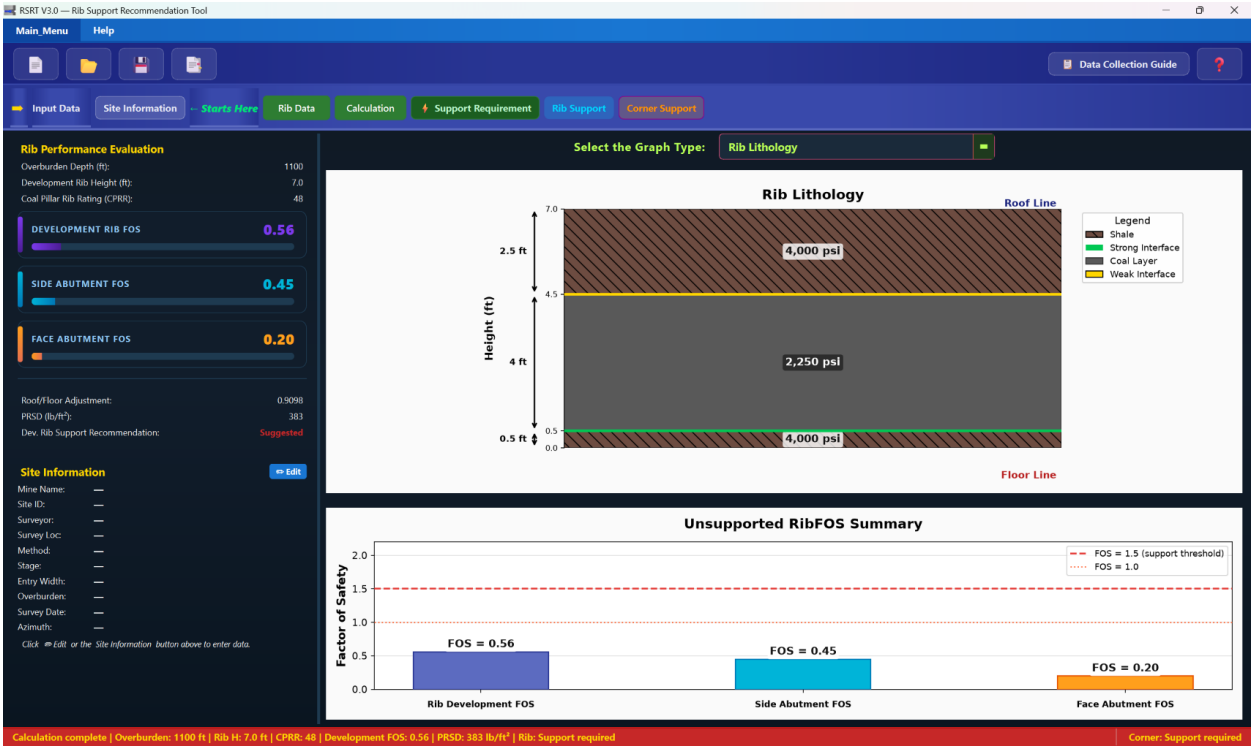


Figure 36: RSRT calculation output for the No. 2 Gas seam case, showing an overburden depth of 1100 ft, a Coal Pillar Rib Rating of 48, and unsupported RibFOS values of 0.56 and 0.45 for the development and side abutment conditions, respectively.

Table 11: RSRT calculation summary for Case 2.

Parameter	Value
Estimated Coal Pillar Rib Rating	48
Development RibFOS, unsupported	0.56
Side abutment RibFOS, unsupported	0.45
Primary Rib Support Density, development (lb/ft^2)	383



Figure 37: RSRT support recommendation for the No. 2 Gas seam case under development loading, showing one fully grouted bolt, 4 to 5 ft long, at 4 to 6 ft spacing.

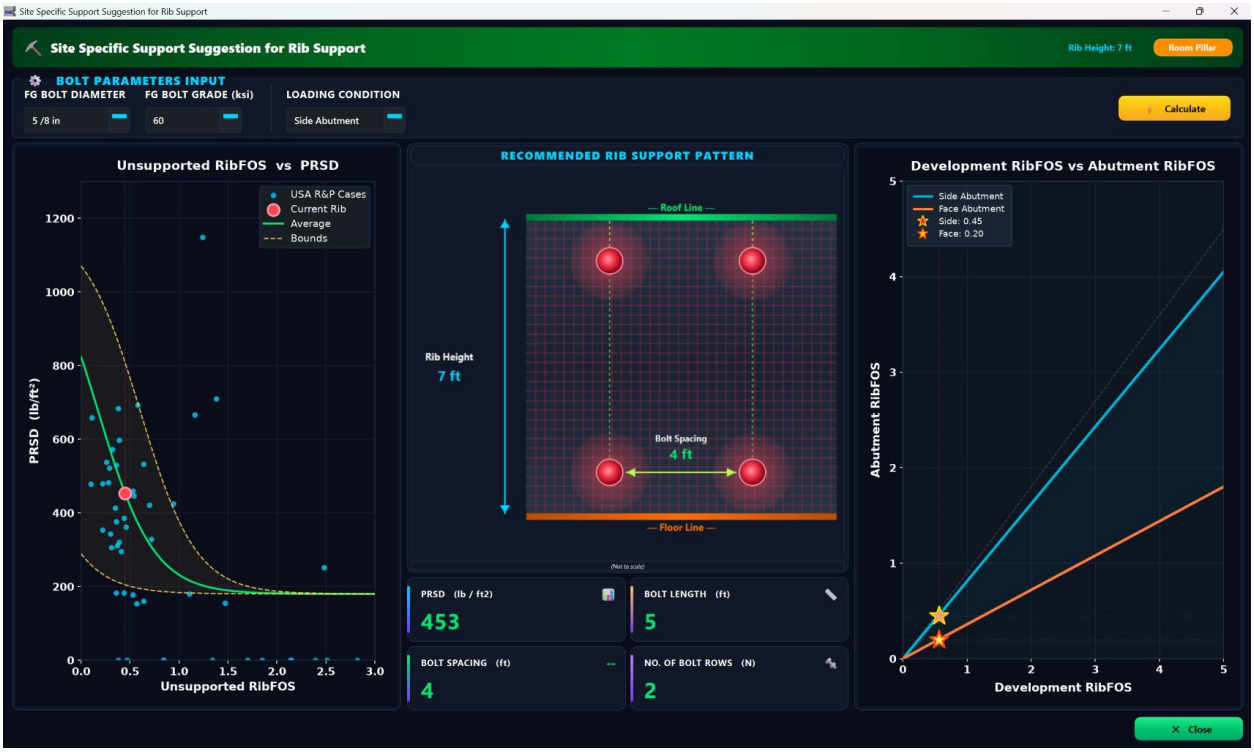


Figure 38: RSRT support recommendation for the No. 2 Gas seam case under side abutment loading, showing two fully grouted bolts, 5 ft long, at 4 ft spacing.

Table 12 provides a comparison between the support pattern used in the field and the recommended support pattern based on the RSRT output.

Table 12: Case 2, No. 2 Gas Seam comparison of the active mine support with the RSRT support recommendation.

Parameter	Active support (mine)	RSRT, development	RSRT, side abutment
Number of bolts	1	1	2
Bolt length (ft)	5	4 to 5	5
Spacing (ft)	8	4 to 6	4
Bolt type	Fully grouted, angled into shale only, none in coal	Fully grouted, installed at mid-rib	Fully grouted, installed in coal unit
Secondary support	Not used	Not required	Not required

For these two field cases, the support recommendations produced by the RSRT tool were consistent with or more extensive than the support practices documented at the selected locations. For the Eagle Seam case, the RSRT primary support recommendation matched the active primary support pattern, while the tool also recommended secondary support. For the No. 2 Gas Seam case, the development recommendation retained a single support row but reduced the spacing and changed the support location, while the side abutment evaluation increased the recommendation to two bolts at 4 ft spacing. The cases demonstrate how the newly incorporated MSI and abutment-loading adjustments affect RSRT outputs under field-derived conditions. They do not constitute comprehensive validation of the RSRT across its full parameter space, particularly because the No. 2 Gas Seam overburden depth and the Eagle Seam shale properties extend beyond the limits of the underlying numerical database. Continued evaluation against additional field cases is therefore needed to assess the RSRT recommendations across a broader range of mining and geological conditions.

4.0. Research Accomplishments

This section summarizes the principal research accomplishments achieved during the project and relates the key findings and outcomes to the specific project objectives.

4.1 Field Data Collection and Monitoring for Coal Rib Stability Research

Field Surveys of Active Coal Mines

As part of this research project, field surveys were completed at 8 underground coal mines covering 7 coal seams and a broad range of rib and pillar-corner conditions. The surveys documented coal rib behavior under varying mining and geological conditions, including overburden depth, rib composition, support practices, multiple-seam interaction, abutment loading, and pillar-corner conditions. These observations expanded the project database of field conditions used to evaluate coal rib behavior and provided field-derived cases for evaluating the expanded coal rib control system and RSRT application.

The information collected from these surveys can be used as calibration data and validation cases, supporting continued numerical model development and future research on coal rib stability.

Field Monitoring

The field monitoring effort produced a coordinated dataset that quantified the evolution of pillar stress-transfer responses, rib deformation, and rib-bolt loading as pillar retreating approached the instrumented pillar. The measurements documented a clear transition from relatively stable development conditions to increased response during retreat. Changes in pillar pressure, rib displacement, and rib-bolt load became evident as the retreat line approached within approximately two breaks. Rib displacement increased approximately fourfold when retreating reached one break away, while bolt loads reached approximately 5,000 lb, or about 25% of the bolt yield capacity. The borehole pressure cells also quantified the spatial variation in stress transfer, with the average pressure change on the crosscut side reaching approximately 500 psi when half of the instrumented pillar had been mined, nearly twice that measured on the entry side.

A principal accomplishment of this effort was the simultaneous quantification of stress transfer, rib deformation, and support demand during the same retreat sequence. The resulting field dataset provides a basis for calibrating and validating future numerical models, evaluating stress-transfer mechanisms during pillar retreating, and assessing rib-support response under changing loading conditions.

4.2 Quantified Effects of MSI and Abutment Loading on RibFOS and Advanced Rib-Corner Stability Analysis

The numerical modeling phase of this project quantified the effects of multiple-seam interaction and abutment loading on RibFOS and extended the established rib-modeling methodology to investigate pillar-corner response and potential support configurations.

To evaluate MSI and abutment loading, more than 400 numerical simulations were completed across representative mining and geological conditions. The MSI study established relationships between MSI-induced vertical stress increases and reductions in RibFOS. The resulting generalized relationship provides a direct connection between the percent vertical stress increase obtained from ACPS and the corresponding RibFOS adjustment used by the coal rib control system.

The abutment-loading study established generalized RibFOS reductions of 19% under side abutment loading and 64% under face abutment loading relative to development conditions. These relationships provide a quantitative basis for accounting for changes in coal rib stability as mining progresses from development to abutment-loading conditions.

The MSI and abutment-loading relationships provide an engineering basis for accounting for these loading conditions in coal rib stability assessments without requiring a separate numerical analysis for each individual application. Their incorporation into the RSRT also allows the relationships to be applied within the existing coal rib control framework.

The project also extended the 2D rib modeling methodology to 3D pillar-corner models and evaluated 10 representative corner scenarios. The models provided initial quantitative insight into the extent of the displacement-defined mobilized zone at pillar corners and the influence of alternative support configurations. Support-pattern exploration showed that increasing support density reduced the mobilized zone in the selected model case, while positioning the denser support closer to the corner further improved the modeled response. Among the initially evaluated support configurations, the asymmetric support pattern produced the greatest reduction in the mobilized zone and provided the basis for preliminary corner-support guidance.

The 3D modeling framework and support-pattern findings provide a foundation for future field-calibrated studies aimed at developing a quantitative rib-corner stability and support-design methodology.

4.3 Expanded the Coal Rib Control System and RSRT for Complex Loading and Rib-Corner Conditions

The project expanded the capabilities of the Rib Support Recommendation Tool (RSRT) to account for MSI effects, side and face abutment loading conditions, and preliminary rib-corner support guidance. The RSRT was also transferred from its original MATLAB-based platform to a Python-based desktop application to improve usability, application workflow, and future expandability.

The relationships used to determine CPRR, development RibFOS, and rib-support recommendations from the previous Alpha Foundation project were retained in the updated RSRT. The new MSI and abutment-loading relationships developed in this project were incorporated as adjustments to development RibFOS. For MSI evaluations, the application uses the percent vertical stress increase obtained from ACPS to determine the applicable RibFOS adjustment. For

abutment loading, the application applies the side- or face-abutment RibFOS multiplier developed from the parametric modeling results. The resulting adjusted RibFOS is then used within the existing RSRT support-recommendation framework.

Preliminary corner-support guidance developed from the 3D modeling study was also incorporated into a separate RSRT interface. This interface allows the user to account for differences between the entry and crosscut rib conditions when applying the asymmetric corner-support configuration explored in this project.

The updated RSRT was evaluated using two field-derived cases representing MSI and side abutment loading conditions. The Eagle Seam case demonstrated how the MSI adjustment changes RibFOS and support requirements under severe multiple-seam conditions, while the No. 2 Gas Seam case demonstrated how the side-abutment adjustment changes the recommended support as loading conditions progress beyond development. These field-case evaluations provided an initial assessment of the newly incorporated RSRT capabilities under documented mine conditions.

The updated Python-based RSRT provides a practical and expandable platform for transferring the engineering relationships developed through this and previous Alpha Foundation projects into mine-design workflows. Its modular structure also provides a foundation for incorporating future advances in coal rib stability, loading effects, and support design as additional field and numerical data become available.

5.0. Publication Record and Dissemination Efforts

Two manuscripts have been prepared from the outcomes of this research and are currently being finalized for submission to peer-reviewed journals. The manuscripts address the project findings on MSI and abutment loading effects on coal rib stability and the 3D rib-corner modeling and support investigation. Following journal publication, the research findings are also planned to be presented at the SME Annual Conference to further disseminate the project outcomes to the mining industry and research community.

A major dissemination outcome of this project is the updated coal rib control system and Python-based RSRT application, which provide a practical means of transferring the engineering relationships and support guidance developed through this and previous Alpha Foundation projects to mine operators and researchers. The field-case evaluations completed in this project provide an initial demonstration of the updated RSRT capabilities for accounting for MSI and abutment loading under documented mine conditions.

Continued development of the RSRT will require interaction with NIOSH and industry partners to evaluate the tool under a broader range of field conditions and obtain direct feedback on its usability, applicability, and support recommendations. This feedback will help identify areas for refinement, guide expansion of the tool's capabilities, and support continued improvement of the underlying coal rib control system. Broader interaction with mine operators and researchers will also facilitate dissemination of the RSRT and its application in coal mine rib stability assessment and support design.

6.0. Conclusions and Impact Assessment

The outcomes of this research have culminated in multiple practical and research outcomes that are expected to improve coal mine health and safety.

Completing field surveys at 8 underground coal mines covering 7 coal seams provided new datasets on field conditions and interactions affecting coal rib stability. These observations expanded the project database of coal rib and pillar-corner behavior under a broad range of mining and geological conditions. The information collected from these surveys can be used as calibration data and validation cases, supporting continued numerical model development and future research on coal rib stability.

Completion of an instrumented pillar study provided deformation, load, and response data on pillar and rib behavior under retreat conditions and quantified the evolution of pillar stress-transfer responses, rib deformation, and rib-bolt loading as pillar retreating approached the instrumented pillar. A principal outcome of the monitoring effort was the simultaneous measurement of stress transfer, rib deformation, and support demand during the same retreat sequence. The resulting field dataset provides a basis for future numerical model calibration and validation and for evaluating stress-transfer mechanisms and rib-support response under changing loading conditions.

This research explicitly linked outputs from the NIOSH-developed ACPS software to the MSI adjustment incorporated into the coal rib control system and RSRT, enabling the effective incorporation of multiple seam interaction effects into rib stability analysis. The percent vertical stress increase obtained from ACPS can therefore be used to adjust development RibFOS within the RSRT, providing a practical connection between coal pillar stability analysis and coal rib stability assessment.

A key finding from the parametric modeling studies for quantifying the effect of multiple seam interactions on rib stability was that the relationship between increasing MSI-induced vertical stress and decreasing RibFOS remained consistent across the three evaluated rib-configuration groups: single-solid coal ribs, ribs with rock partings, and ribs with weak bedding planes. This consistency supported pooling the numerical results to develop a generalized relationship between percent vertical stress increase and the RibFOS adjustment within the modeled range. This relationship facilitates incorporation of MSI effects into the coal rib control system without requiring a separate numerical analysis for each site-specific application.

The outcomes of the parametric studies on quantifying abutment loading conditions established generalized reductions in development RibFOS of 19% under side abutment loading and 64% under face abutment loading. These relationships were incorporated into the RSRT to account for changes in rib stability as mining conditions progress beyond development. Field-case evaluations representing MSI and side abutment loading provided an initial assessment of these newly incorporated RSRT capabilities under documented mine conditions. These evaluations should not be interpreted as comprehensive validation of the RSRT across its full parameter space.

The study successfully explored coal rib corner stability and gained critical insights into interactions between support design and corner behavior. Within the support configurations evaluated, increasing support density produced a greater reduction in the displacement-defined mobilized zone, while positioning the denser support closer to the corner further improved the modeled response. The asymmetric support configuration produced the greatest reduction among the initially evaluated support patterns and provided the basis for preliminary rib-corner support guidance.

Initial modeling efforts of coal rib corner stability analysis identified limitations in the numerical methodology for evaluating support effects for some rib configurations. In addition, the lack of direct field measurements of pillar-corner response prevented explicit calibration of the corner models. Therefore, the corner findings should be considered preliminary and provide a foundation for future field-calibrated studies aimed at developing a quantitative rib-corner stability and support-design methodology.

Enhancing the capabilities of the RSRT by integrating multiple seam interactions, abutment loading, and preliminary rib-corner support guidance, together with transferring the application from MATLAB to a Python-based platform, expanded the practical capabilities of the coal rib control system. The updated RSRT provides an engineering platform for applying the relationships developed through this and previous Alpha Foundation projects and for incorporating future improvements as additional field and numerical data become available. Continued evaluation and feedback from NIOSH, industry partners, and mine operators will be important for further refinement, expansion, and dissemination of the tool.

7.0. Recommendations for Future Work

The work completed in this study on exploring coal rib corner stability and support is a preliminary effort using available data and methodologies, but more work is needed to quantify corner stability and develop validated corner-support guidance. Methodological limitations in the numerical modeling approach used in this study and the lack of direct field measurements of pillar-corner response limited the ability to explicitly quantify and calibrate corner stability. Future work should include direct monitoring of pillar-corner response under representative mining and geological conditions. These data should be used to calibrate and validate 3D corner models and support development of a quantitative corner-stability metric and engineering-based corner-support design methodology. Additional numerical work should also evaluate alternative discontinuum modeling approaches and a broader range of corner geometries, loading conditions, and support configurations.

Interactions between MSI and abutment loading conditions need to be explored and quantified to fully capture the effects these conditions have on rib stability in complex coal mining environments. The present study evaluated these loading effects separately. Future numerical studies should therefore investigate their combined influence on RibFOS and determine whether the adjustment relationships developed in this project remain applicable when MSI and abutment loading occur simultaneously. Furthermore, the upper limit of vertical stress increases due to MSI should be expanded to account for higher overburden-interburden ratios and more severe MSI conditions occasionally observed in the field. Additional simulations beyond the 10% to 90% vertical stress increase range evaluated in this study would allow the MSI relationship to be extended without relying on extrapolation of the current regression equation.

Evaluations of the recommended support designs provided by the RSRT application are necessary to quantify the performance of RSRT-based rib support recommendations relative to existing mine practices. This should be achieved through in-depth field monitoring studies conducted at operating mine sites with various coal rib conditions, where support system designs are implemented and evaluated directly based on outputs from the RSRT application. These field trials should document rib response, support loading, and changes in rib condition over time so that the recommendations can be evaluated under actual operating conditions. Continued interaction with mine operators and other industry users should also be used to identify limitations, obtain feedback on usability and implementation, and guide expansion and improvement of the RSRT.

Future research should expand the coal rib control system's capabilities to include surrogate modeling tools that allow coal mine operators to predict high rib deformation and unstable rib zones without using numerical modeling tools. Such models could use the numerical and field datasets developed through this and previous research to provide rapid estimates of rib response for site-specific mining and geological conditions. Incorporating this functionality into the coal rib control system will provide coal mine operators with additional engineering support for identifying locations where increased rib deformation or instability may occur and where support may need to be strengthened.

8.0. Acknowledgment

The research team sincerely thanks Dr. Khaled M. Mohamed, Dr. Yuting Xue, James Addis, and Mark Mazzella from the NIOSH Pittsburgh Branch for their invaluable help during the fieldwork and monitoring phases of this study. Furthermore, we express our gratitude and appreciation to our industry partners, Blackhawk Mining LLC, Core Natural Resources, and Peabody Energy, for granting us access to their mine sites.

9.0. References

Barczak, T. M., Esterhuizen, G. S., Ellenberger, J., & Zhang, P. (2008). A first step in developing standing roof support design criteria based on ground reaction data for Pittsburgh seam longwall tailgate support. In Proceedings of the 27th International Conference on Ground Control in Mining,

Guner, D., Nowak, S., Sherizadeh, T., Sunkpal, M., Mohamed, K., & Xue, Y. (2023). Review of current coal rib control practices. *Underground Space*, *9*, 53-75. https://doi.org/10.1016/j.undsp.2022.04.011

Guner, D., Sherizadeh, T., Nowak, S., Karadeniz, K. E., & Sunkpal, M. (2023). Distinct element analysis for the effectiveness of preliminary coal pillar rib support systems based on the strength reduction method using coal mass constitutive model. *Mining, Metallurgy & Exploration*, *40*(5), 1535-1546.

Itasca Consulting Group, I. (2021). *3DEC-Three-Dimensional Distinct Element Code, Ver. 7.0.* Itasca. https://docs.itascasoftware.com/flac3d700/3dec/docproject/source/3dechome.html?node6309

Jones, T. H., Klemetti, T. M., & Mohamed, K. M. (2014, 07/29/2014). Investigating the Contributing Factors to Rib Fatalities Through Historical Analysis. International Conference on Ground Control in Mining,

Liu, H., Sang, S., Xue, J., Wang, G., Xu, H., Ren, B., Liu, C., & Liu, S. (2016). Characteristics of an in situ stress field and its control on coal fractures and coal permeability in the Gucheng block, southern Qinshui Basin, China. *Journal of Natural Gas Science and Engineering*, *36*, 1130-1139.

Mark, C. (2021). An updated empirical model for ground control in U.S. multiseam coal mines. *International Journal of Mining Science and Technology*, *31*(2), 163-174. https://doi.org/10.1016/j.ijmst.2020.12.024

Mark, C., & Agioutantis, Z. (2019). Analysis of coal pillar stability (ACPS): A new generation of pillar design software. *International Journal of Mining Science and Technology*, *29*(1), 87-91. https://doi.org/10.1016/j.ijmst.2018.11.007

Mark, C., Chase, F. E., & Pappas, D. M. (2007a). *Analysis of Multiple Seam Stability*. https://stacks.cdc.gov/view/cdc/161081

Mark, C., Chase, F. E., & Pappas, D. M. (2007b). Multiple-seam mining in the United States: design based on case histories. Proceedings on the New Technology for Ground Control in Multiple Seam Mining,

Mohamed, K., Sears, M., Guner, D., Nowak, S., Kirmaci, A., & Sherizadeh, T. (2023). *Coal Pillar Rib Stability: A Regression Model Based on Distinct Element Method* proceedings of the 42nd international conference on ground control in mining,

Mohamed, K., Van Dyke, M., Rashed, G., & Kimutis, R. (2021b). *Analyzing rib stability and support using a coal pillar rib rating* proceedings of the 40th international conference on ground control in mining,

Mohamed, K. M., Cheng, Z., & Rashed, G. (2019). Coal rib stability based on the strength reduction of the coal mass model. ARMA US Rock Mechanics/Geomechanics Symposium,

Mohamed, K. M., Murphy, M. M., Lawson, H. E., & Klemetti, T. (2016). Analysis of the current rib support practices and techniques in U.S. coal mines. *International Journal of Mining Science and Technology*, *26*(1), 77-87. https://doi.org/10.1016/j.ijmst.2015.11.014

Mohamed, K. M., Rashed, G., Rusnak, J. A., Sears, M. M., & Van Dyke, M. A. (2018, 02/25/2018). *Calibration of a Coal-Mass Model Using An In Situ Coal Pillar Strength Study* SME Annual Meeting, Minneapolis, MN.

MSHA. (2020). *Handbook Series: Roof Control Plan and Ground Support Review Procedures.* (Vol. PH20-V-2). U.S. Department of Labor Mine Safety and Health Administration.

NIOSH. (2019). *Mining Program Strategic Plan*. https://archive.cdc.gov/www_cdc_gov/niosh/mining/strategicplan/MiningStrategicPlan2019-2024.html

Rashed, G., Barton, T., Sears, M., Van Dyke, M., & Mohamed, K. (2018). Estimation of the intact strength of coal using indirect methods. In Proceedings of the 37th International Conference on Ground Control in Mining, Morgantown, West Virginia.

Saptono, S., Kramadibrata, S., & Sulistianto, B. (2013). Using the Schmidt Hammer on Rock Mass Characteristic in Sedimentary Rock at Tutupan Coal Mine. *Procedia Earth and Planetary Science*, *6*, 390-395. https://doi.org/10.1016/j.proeps.2013.01.051

Sherizadeh, T. (2023). *Reducing Rib Hazards in Underground Coal Mines by Improvement of the Coal Pillar Rib Rating (CPRR) System* (Final Technical Report (AFCRFP20-112)).

Sherizadeh, T., Guner, D., & Kirmaci, A. (2024). *Improvement of Rib Support Design Utilizing Recent Advancements of the Coal Pillar Rib Rating (CPRR) System* (Third Interim Report (AFCTG22-152)).

Sinha, S., & Walton, G. (2019). Understanding continuum and discontinuum models of rock-support interaction for excavations undergoing stress-induced spalling. *International Journal of Rock Mechanics and Mining Sciences*, *123*. https://doi.org/10.1016/j.ijrmms.2019.104089

Zhang, P., Mohamed, K. M., & Trackemas, J. (2017). Coal Rib Failure and Support in Longwall Gate Entries. 51st U.S. Rock Mechanics/Geomechanics Symposium,

Zipf, R. K. (2005). Failure mechanics of multiple seam mining interactions. Proceedings of the 24th International Conference on Ground Control in Mining, Morgantown, West Virginia.